



**HAL**  
open science

# Bilateral control of interceptive saccades: evidence from the ipsipulsion of vertical saccades after caudal fastigial inactivation

Clara Bourrelly, Julie Quinet, Laurent Goffart

► **To cite this version:**

Clara Bourrelly, Julie Quinet, Laurent Goffart. Bilateral control of interceptive saccades: evidence from the ipsipulsion of vertical saccades after caudal fastigial inactivation. *Journal of Neurophysiology*, 2021, Control of movement, 125 (6), pp.2068-2083. 10.1152/jn.00037.2021 . hal-03168070v2

**HAL Id: hal-03168070**

**<https://hal.science/hal-03168070v2>**

Submitted on 2 Apr 2021

**HAL** is a multi-disciplinary open access archive for the deposit and dissemination of scientific research documents, whether they are published or not. The documents may come from teaching and research institutions in France or abroad, or from public or private research centers.

L'archive ouverte pluridisciplinaire **HAL**, est destinée au dépôt et à la diffusion de documents scientifiques de niveau recherche, publiés ou non, émanant des établissements d'enseignement et de recherche français ou étrangers, des laboratoires publics ou privés.

1 Bilateral control of interceptive saccades: evidence from  
2 the ipsipulsion of vertical saccades after caudal fastigial  
3 inactivation

4

5 Clara Bourrelly\*, Julie Quinet and Laurent Goffart\*

6 Aix Marseille Université, Centre National de la Recherche Scientifique,

7 Institut de Neurosciences de la Timone, Marseille, France.

8

9 Laurent Goffart : <https://orcid.org/0000-0001-8767-1867>

10 Julie Quinet : <https://orcid.org/0000-0003-3043-3424>

11 Title for running head: Neural control of interceptive saccades

12

13 \*: C. Bourrelly and L. Goffart contributed equally to this work.

14 Address for correspondence:

15 Laurent Goffart, PhD,

16 E-mail: [laurent.goffart@univ-amu.fr](mailto:laurent.goffart@univ-amu.fr)

17 Institut de Neurosciences de la Timone, Campus de Sante, 27 Bd Jean Moulin, 13385 Marseille

18 cedex 5, France.

19

20

21 **Abstract (219 words <= 250 words)**

22 The caudal fastigial nuclei (cFN) are the output nuclei by which the medio-posterior cerebellum  
23 influences the production of saccades toward a visual target. On the basis of the organization  
24 of their efferences to the premotor burst neurons and the bilateral control of saccades, the  
25 hypothesis was proposed that the same unbalanced activity accounts for the dysmetria of all  
26 saccades during cFN unilateral inactivation, regardless of whether the saccade is horizontal,  
27 oblique, or vertical. We further tested this hypothesis by studying, in two head-restrained  
28 macaques, the effects of unilaterally inactivating the caudal fastigial nucleus on saccades  
29 toward a target moving vertically with a constant, increasing or decreasing speed. After local  
30 muscimol injection, vertical saccades were deviated horizontally toward the injected side with  
31 a magnitude that increased with saccade size. The ipsipulsion indeed depended upon the tested  
32 target speed, but not its instantaneous value because it did not increase (decrease) when the  
33 target accelerated (decelerated). By subtracting the effect on contralesional horizontal saccades  
34 from the effect on ipsilesional ones, we found that the net bilateral effect on horizontal saccades  
35 was strongly correlated with the effect on vertical saccades. We explain how this correlation  
36 corroborates the bilateral hypothesis and provide arguments against the suggestion that the  
37 instantaneous saccade velocity would somehow be “encoded” by the discharge of Purkinje cells  
38 in the oculomotor vermis.

39

40 **NEW & NOTEWORTHY (73 <= 75 words)**

41 Besides causing dysmetric horizontal saccades, unilateral inactivation of caudal fastigial  
42 nucleus causes an ipsipulsion of vertical saccades. This study is the first to quantitatively  
43 describe this ipsipulsion during saccades toward a moving target. By subtracting the effects on  
44 contralesional (hypometric) and ipsilesional (hypermetric) horizontal saccades, we find that this  
45 net bilateral effect is strongly correlated with the ipsipulsion of vertical saccades, corroborating  
46 the suggestion that a common disorder affects all saccades.

47

## 48 **Introduction**

49           Saccades are rapid changes in eye orientation whose time course is characterized by an  
50 interval during which the rotation speed increases to a maximum (acceleration) followed by an  
51 interval during which it returns to zero (deceleration). Starting with the eyes centered in the  
52 orbits, the changes in the contraction of lateral and medial recti muscles rotate the eyes  
53 horizontally whereas combined changes in the contraction of superior and inferior recti  
54 muscles, and the superior and inferior oblique muscles rotate them vertically (Robinson 1975).  
55 During vertical saccades, the tension in muscles involved in horizontal rotations exhibit a  
56 transient small reduction at the level of medial recti (Miller and Robins 1992). A burst of spikes  
57 from motoneurons causes the phasic contraction of agonist muscles while the relaxation of  
58 antagonist muscles is enabled by a pause of motoneurons which innervate them (Fuchs and  
59 Luschei 1970; Robinson 1970; Schiller 1970). Premotor commands for horizontal and vertical  
60 eye rotations originate in distinct regions of the reticular formation: burst neurons in the  
61 pontomedullary reticular formation drive horizontal saccades whereas those controlling vertical  
62 saccades are located in the rostral midbrain tegmentum (Fuchs et al. 1985; Hepp et al., 1989;  
63 Horn 2006; Moschovakis et al. 1996).

64           Robinson and Fuchs (2001) proposed that these populations of premotor neurons and  
65 the time course of saccades are under the control of neurons in the medio-posterior cerebellum:  
66 burst neurons in the contralateral caudal fastigial nucleus (cFN) would support the acceleration  
67 of saccades while those in the ipsilateral cFN would help their deceleration. This biphasic  
68 pattern was suggested by the delay between the peaks of cFN discharge during contralateral  
69 and ipsilateral saccades (Fuchs et al. 1993; Ohtsuka and Noda 1991; Kleine et al. 2003).  
70 Moreover, after unilateral cFN inactivation, contralesional saccades are hypometric and exhibit  
71 lower peak velocity whereas ipsilesional saccades are hypermetric with a longer deceleration

72 (Buzunov et al. 2013; Goffart et al. 2004). Thus, it was suggested that a shift of activity from  
73 the contralateral to the ipsilateral cFN would guide the trajectory of saccades (Optican 2005).

74 Numerous observations lead to questioning this isomorphism which was assumed  
75 between the brainstem activity and the kinematics of saccades. Firstly, Davis-Lopez de  
76 Carrizosa et al. (2011) showed that a model factoring muscle tension and its first derivative  
77 accounted for the firing rate of motoneurons better than a model factoring eye position and its  
78 first and second derivatives (velocity and acceleration). Secondly, the resemblance between the  
79 firing rate of premotor burst neurons and saccade instantaneous velocity (see for example Fig.  
80 5B of Cromer and Waitzman (2007)) disappears when the spikes are not convolved with a  
81 Gaussian kernel (see Figs. 2 and 3 in Hu et al. (2007); Fig. 3C in Sparks & Hu (2006) and Fig.  
82 4 in van Gisbergen et al. (1981)). Thirdly, the inspection of cFN bursts reveals that the transition  
83 between the activity of the left and right cFN is not as sharp as the separation between the  
84 acceleration and deceleration phases. In fact, the bursts in the two nuclei largely overlap around  
85 the time of saccade peak velocity (Kleine et al. 2003). Moreover, some neurons burst after  
86 saccade onset during large contralateral head unrestrained gaze shifts, casting doubt on the  
87 cFN's role in accelerating saccades (Fuchs et al. 2010). Involvement in only decelerating  
88 ipsilateral saccades is also called into question by the changes in the acceleration of saccades  
89 after cFN inactivation (Buzunov et al. 2013; Quinet and Goffart 2007). Finally, a horizontal  
90 deviation (ipsipulsion) affects the full time course of vertical saccades, including both  
91 acceleration and deceleration, following unilateral cFN inactivation (Goffart et al. 2004;  
92 Iwamoto and Yoshida 2002; Quinet and Goffart 2007).

93 The hypothesis that cFN activity helps to accelerate contralateral horizontal saccades  
94 and to decelerate ipsilateral ones does not explain why vertical saccades exhibit this ipsipulsion.  
95 Robinson et al. (1993) proposed a different explanation: “during saccades to vertical targets,  
96 there is activity in the horizontal burst generator on one side that is not balanced by activity on

97 the other. Such unbalanced activity might arise because in the normal animal, caudal fastigial  
98 neurons on each side burst at about the same time during vertical saccades”. Emphasizing the  
99 organization of cFN efferences to premotor burst neurons (Sparks and Barton 1993) and the  
100 bilateral control of saccades (van Gisbergen et al. 1981), Goffart et al. (2004) went further by  
101 proposing that the unbalanced activity accounts for the dysmetria of all saccades during cFN  
102 unilateral inactivation, regardless of whether the saccade is horizontal, oblique, or vertical.  
103 According to this bilateral hypothesis, both cFN influence the premotor process, from saccade  
104 onset to saccade end. Regardless of its direction, the saccade is influenced by the discharge  
105 from both cFN. If the causes are the same, the ipsipulsion of vertical saccades should be  
106 correlated with the dysmetria of horizontal (ipsilesional and contralesional) saccades; this  
107 inference is not deducible from the scheme proposed by Robinson and Fuchs (2001). In the  
108 present study, we characterize the ipsipulsion of vertical saccades, and confirm this prediction  
109 using saccades toward a moving target as a probe. We investigated such saccades because they  
110 offer the methodological advantage of enabling to vary both target eccentricity and the saccade  
111 amplitude more easily than saccades toward static targets. Goffart et al. (2004) indeed found  
112 that the magnitude of the ipsipulsion increased when target eccentricity (see also Iwamoto and  
113 Yoshida 2002) or saccade duration increased. Which of these features (target eccentricity or  
114 saccade duration) determines the size of the horizontal error could not be determined from their  
115 data. Our results do not support a link between the ipsipulsion and saccade duration because  
116 across all our testing conditions, its magnitude was less frequently dependent upon the duration  
117 than upon the amplitude of vertical saccades.

## 118 **Materials and Methods**

119           The materials and methods used in this work are identical to those described in Burrelly  
120 et al. (2018a, b) and comply with the ARRIVE (Animal Research: Reporting of In Vivo  
121 Experiments) guidelines. We will remind them only briefly.

### 122 *Subjects and surgical procedures*

123           Two adult male rhesus monkeys (*Macaca mulatta*, 11-12 kg) participated in this study.  
124 Their eye movements were recorded with the electromagnetic induction technique. Training to  
125 the eye movement tasks started after full recovery (> 1 month after surgery). A craniotomy was  
126 made to permit the electrophysiological localization of saccade-related neurons in both fastigial  
127 nuclei. The surgical procedures and experiments were performed in accordance with the  
128 guidelines from the French Ministry of Agriculture and the European Community, after  
129 approval from the Regional Ethics Committee (authorization # A13/01/13). Care and  
130 maintenance of animals were made under the auspices of a veterinarian and the assistance of  
131 animal facilities staff.

### 132 *Eye movement recording and visual stimulation*

133           During the experimental sessions, the monkeys were seated in a chair with their head  
134 restrained, facing a LCD video monitor (Samsung SyncMaster, P227f; 1,280 × 1,024 pixels,  
135 100-Hz refresh rate, 39 × 29 cm) located at a viewing distance of 38 cm. The visual target was  
136 a Gaussian blurred white disk of 0.4° diameter displayed over a gray background. Eye  
137 movements were measured with a phase-angle detection system (CNC Engineering, 3-ft. coil  
138 frame) and voltage signals encoding the horizontal and vertical positions of one eye were  
139 sampled at 500 Hz. The triggering of stimuli, the on-line recording of the oculomotor  
140 performance and the data acquisition were controlled by a PC using the Beethoven software

141 package (Ryklin Software). Eye position signals were calibrated by having the animal fixate  
142 stationary targets presented at  $\pm 16^\circ$  along the horizontal or vertical meridians.

### 143 *Oculomotor tests*

144 The experiments were performed more than one year after the monkeys were tested and  
145 trained to make saccades toward moving targets (Quinet and Goffart 2015; Burreilly et al.  
146 2014, 2016). Each experiment consisted of several pre-injection (control) sessions and one post-  
147 injection session. During the control sessions, the eye movements were recorded with a series  
148 of trials performed over 3-4 successive days before the injection whereas the post-injection  
149 session consisted of recordings made during trials collected approximately 30-50 minutes after  
150 the muscimol was injected in the cFN (after removing the cannula from the brain and recording  
151 saccades toward static targets). Each trial started with a brief tone followed by the appearance  
152 of a target at the center of the visual display (straight ahead). After the monkey directed its gaze  
153 toward its location within a surrounding invisible window ( $12^\circ$  centered on the target) and for  
154 a variable interval (ranging from 750 to 1500 ms by increments of 250 ms), the central target  
155 moved centrifugally along a cardinal (horizontal and vertical meridians) or oblique axis with a  
156 constant speed ( $10^\circ/\text{s}$  during 1,200 ms,  $20^\circ/\text{s}$  during 600 ms or  $40^\circ/\text{s}$  during 300 ms), or with an  
157 increasing (from 0 to  $40^\circ/\text{s}$  during 600 ms) or decreasing speed (from 40 to  $0^\circ/\text{s}$  during 600 ms).  
158 The different types of target speed were tested in separate blocks of trials. Within each block,  
159 the direction of target motion (cardinal or oblique) was pseudo-randomly selected (one out of  
160 eight possible directions) in order to prevent the generation of anticipatory eye movements. The  
161 monkeys' task was to track the target until the location where it disappeared at the end of the  
162 trial. The fixation constraints for controlling the accuracy of eye movements were relaxed with  
163 respect to requirements for obtaining their reward. Indeed, the monkeys had to direct their gaze  
164 within a large invisible window around the moving target ( $12^\circ$  centered on the moving target).  
165 Otherwise, the trial was aborted and a new trial started. Our recordings show that these relaxed

166 constraints do not incite monkeys to perform inaccurate saccades (see Figs. 3, 5, 7 and 9 in  
167 Bourrelly et al. 2018; see also Fleuriet and Goffart 2012; Quinet and Goffart 2015). Each  
168 session (lasting 1 to 2 hours) was composed of different blocks of trials whose number  
169 depended upon the monkey's motivation. Water-deprived in their home cage, the monkeys  
170 obtained the water they need during daily sessions. A session ended when they stopped fixating  
171 the central target for more than ten successive trials.

### 172 *Muscimol injection*

173 A thin cannula (beveled tip) was connected to a Hamilton syringe with polyethylene  
174 tubing. We filled the inner volume with a saline solution of muscimol (2  $\mu\text{g}/\mu\text{l}$ ). The cannula  
175 was lowered through the same guide tube used during the electrophysiological sessions and  
176 aimed at the fastigial region where neurons emitted bursts during saccades. Small volumes (0.2–  
177 1.1  $\mu\text{l}$ ) of muscimol were injected by small pulses over a time interval of approximately 15  
178 minutes. The injected volume was checked by the displacement of a meniscus of air in the  
179 tubing (1 mm corresponding to 0.1  $\mu\text{l}$ ). Before starting the recording of eye movements toward  
180 a moving target, saccades toward static targets were recorded for approximately 15-30 minutes  
181 in order to complete a companion study (Goffart et al. 2005, 2017b; Quinet and Goffart 2016).  
182 During the muscimol sessions, the blocks that tested the tracking of accelerating or decelerating  
183 targets were always the last ones.

### 184 *Data analysis*

185 The results presented in this paper concern the data obtained before and after ten  
186 unilateral muscimol injections performed in the cFN of two monkeys (6 injections in monkey  
187 A, 4 in monkey Bi). For each experiment, the performance after muscimol injection was  
188 compared with that recorded during the 3-4 preceding control daily sessions. No noticeable  
189 difference was observed between the responses collected during the pre-injection sessions, so

190 movements were pooled together to include some day-to-day variability in our control dataset.  
191 For each monkey, we injected muscimol into the left cFN in half of the experiments and in the  
192 right cFN in the others. All data were digitized on-line and analyzed off-line using a custom-  
193 made software program that detected the onset and offset of the horizontal and vertical  
194 components of saccades on the basis of a velocity threshold ( $30^\circ/\text{s}$ ). The results of this automatic  
195 detection were checked by inspecting each trial individually, and were adjusted manually when  
196 necessary. The present study describes the effect of unilateral cFN inactivation on the  
197 interceptive saccades made in response to the target when it moved along the vertical meridian.  
198 The effects of fastigial inactivation on movements toward the horizontally moving target were  
199 thoroughly described elsewhere (Bourrelly et al. 2018a, b). The interceptive saccade  
200 corresponds to the first saccade made from a static target toward the target after the onset of its  
201 motion. To make sure that the interceptive saccade was not triggered prematurely, those with  
202 latency  $< 80$  ms were excluded from analysis (0.3% of the total number of trials). The Statistica  
203 software (Statsoft) was used for statistical analyses and figure illustrations. Statistical  
204 significance threshold was set to P-value  $< 0.05$ . Because the size of deficits could differ  
205 between different injections, the mean values of the pre- and post-injection movements were  
206 compared with the non-parametric Wilcoxon test (for paired comparison). Thus, our main  
207 conclusions are based on the systematic effects that were revealed by this overall comparison  
208 across different experiments. The correlations between different behavioral measurements were  
209 evaluated with the (parametric) Bravais-Pearson test whereas the correlation between a  
210 behavioral parameters and the target speed was evaluated with the non-parametric Spearman  
211 test.

## 212 **Results**

### 213 **Figure 1 approximately here**

214 Figure 1 illustrates with a few selected trials how a unilateral injection of muscimol in the cFN  
215 affects the eye movements made in response to a centrifugal target moving at a constant speed  
216 ( $20^\circ/\text{s}$ ) along the vertical meridian. The time course of the horizontal (top row) and vertical  
217 (bottom row) components is shown for movements produced before (gray) and after muscimol  
218 injection (black) in the left (A and B: experiments A2 and A3 in monkey A) or right cFN (C:  
219 experiment Bi9 in monkey Bi). As described elsewhere (Guerrasio et al. 2010), inactivation of  
220 cFN caused a fixation offset toward the injected side. Most starting eye positions were shifted  
221 to the right after muscimol injection in the right cFN (see black arrow in C) and to the left after  
222 muscimol injection in the left cFN (black arrow in A). The ipsilesional offset was not observed  
223 on every trial. We show examples (recorded during the experiments A2 and A3) in which the  
224 saccades were initiated from positions near the vertical meridian (horizontal position values  
225 close to zero in the upper graphs) but below the horizontal meridian (negative values of vertical  
226 position in the lower graphs). In addition to altering gaze direction during fixation, unilateral  
227 cFN inactivation also perturbed vertical saccades. Their trajectory was deviated horizontally  
228 toward the injected side, regardless of whether the target moved upward or downward. In the  
229 following paragraphs, after describing the velocity of their vertical component, we describe the  
230 ipsipulsion that alters the trajectory of vertical saccades.

### 231 **Figure 2 approximately here**

232 As for horizontal saccades (see Fig. 2 in Bourrelly et al. 2018a), muscimol injection in  
233 the cFN barely affected the vertical velocity of saccades. Figure 2 illustrates the vertical  
234 amplitude-peak velocity relationship for four different experiments (two per monkey; A and B:  
235 experiments A2 and A3 in monkey A; C and D: Bi7 and Bi8 in monkey Bi). The peak velocity

236 values are plotted for all upward and downward saccades (positive and negative amplitude  
237 values, respectively) made in response to the different target speeds. When we consider  
238 saccades of comparable vertical amplitude, we can see that the peak velocity is similar between  
239 the pre and post-injection movements.

240 **Figure 3 approximately here**

241 Figure 3 describes the landing position and time of interceptive saccades made toward  
242 a target moving with a constant speed ( $20^\circ/\text{s}$ ) along the vertical meridian (black: upward  
243 motion, gray: downward). For three different experiments (A3 and Bi7: left cFN inactivation;  
244 Bi9: right cFN inactivation), the vertical (top row) and horizontal (bottom row) landing  
245 positions are plotted as a function of their times relative to target motion onset. During the  
246 control sessions (open squares), the vertical landing position increased as the landing time  
247 increased, and the saccades were directed toward locations close to the physical target  
248 (represented by the dashed lines). After muscimol injection (filled squares), the vertical landing  
249 positions still increased as the landing time increased, regardless of the motion direction. The  
250 overlap between pre- and post-injection data points indicates that unilateral cFN inactivation  
251 did not noticeably affect the vertical component of interceptive saccades. Similar findings were  
252 found with respect to saccades toward a static target (Goffart et al. 2004). By contrast, the  
253 horizontal landing positions changed after muscimol injection. While they were scattered along  
254 the vertical meridian (position values close to zero) during the control sessions, their  
255 distribution was shifted toward the injected side after muscimol injection (to the left in  
256 experiments A3 and Bi7, to the right in experiment Bi9). This effect is rather small in  
257 experiment A3 (B: mean  $\pm$  standard deviation values changing from  $-0.1 \pm 0.3^\circ$  to  $-0.5 \pm 0.4^\circ$   
258 after muscimol injection), but the change of horizontal position was much larger in experiments  
259 Bi7 (D: from  $0.0 \pm 0.3^\circ$  to  $-3.5 \pm 1.6^\circ$ ), with Bi9 displaying intermediate values (F: from  $0.3 \pm$   
260  $0.4^\circ$  to  $2.0 \pm 0.7^\circ$ ). Regardless of whether the target moved upward (black symbols) or

261 downward (gray symbols), the horizontal landing position was always shifted toward the  
262 injected side. The size of the ipsipulsion was, in some cases, relatively constant (as in B) or  
263 increased with the landing time (as in D). It is worth noting that the hypermetria of ipsilesional  
264 horizontal saccades was relatively small during experiment A3 whereas it was larger during  
265 experiments Bi7 and Bi9 (see Figures 7 and 10 in Bourrelly et al. 2018a). In summary, an  
266 ipsilesional deviation was observed in the trajectory of vertical saccades during cFN  
267 inactivation. The magnitude of the ipsipulsion varied between experiments, but as we will show,  
268 it is correlated to the magnitude of the dysmetria that impairs the horizontal saccades.

269 To quantify the accuracy of vertical saccades, we calculated for each component the  
270 ratio of landing position to landing time. This parameter (called position/time landing)  
271 characterizes both spatial *and* temporal aspects of saccades made toward a moving target  
272 (Bourrelly et al. 2018a). When we consider saccades toward a target moving along the vertical  
273 meridian, the values of vertical position/time landing are expected to be close to the target speed  
274 if gaze lands next to the target location. A ratio larger than the target speed indicates an  
275 overshoot (too large amplitude) whereas a smaller value means an undershoot (too small  
276 amplitude). Concerning the horizontal component, if gaze lands close to the target, its value is  
277 expected to be close to zero because the target does not move horizontally. We will use the  
278 convention that a positive horizontal ratio indicates an ipsilesional deviation whereas a negative  
279 value is the signature of a contralesional deviation.

280 **Figure 4 approximately here**

281 Figure 4 shows the average vertical position/time landing relationships for each monkey  
282 and each experiment in which the target moved at constant speed. During the control sessions,  
283 the values were close to the target speed ( $11.2 \pm 1.3$ ,  $21.9 \pm 2.0$  and  $38.9 \pm 4.6$  °/s for the 10, 20  
284 and 40 °/s targets, respectively). After muscimol injection, these ratios were larger ( $12.3 \pm$

285 3.8°/s,  $24.3 \pm 4.0^\circ/\text{s}$  and  $44.2 \pm 6.3^\circ/\text{s}$  for the 10, 20 and 40 °/s targets, respectively) (Fig. 4A).  
286 This increase was small but statistically significant (Wilcoxon test, all P values < 0.05). A  
287 stronger affect was observed in the horizontal component of vertical saccades. Figure 4B shows  
288 the average horizontal position/time landings for each tested constant speed, in each experiment  
289 and both monkeys. After muscimol injection, the horizontal position/time landings increased  
290 from  $0.0 \pm 0.7^\circ/\text{s}$  (range:  $-1.1 - 1.6^\circ/\text{s}$ ) to  $5.4 \pm 3.6^\circ/\text{s}$  (range:  $0.8 - 12.1^\circ/\text{s}$ ) when the target  
291 speed was 10°/s, from  $0.0 \pm 1.1^\circ/\text{s}$  (range:  $-2.6 - 2.9^\circ/\text{s}$ ) to  $8.0 \pm 4.9^\circ/\text{s}$  (range:  $1.8 - 18.6^\circ/\text{s}$ )  
292 with the 20°/s target and from  $-0.2 \pm 1.6^\circ/\text{s}$  (range:  $-2.5 - 2.9^\circ/\text{s}$ ) to  $12.0 \pm 7.6^\circ/\text{s}$  (range:  $3.1 -$   
293  $24.2^\circ/\text{s}$ ) with the 40°/s target. The ranges of mean values and the examination of data points in  
294 Fig 4B indicate more variability after muscimol injection than before (see the scattering toward  
295 more positive values; note also the different scales for the x and y axes). During the control  
296 sessions, the average horizontal position/time landings were close to zero (grand averages =  
297 0.0, 0.0 and  $-0.2^\circ/\text{s}$  for the 10, 20 and 40°/s target, respectively; all monkeys considered). After  
298 muscimol injection, the values were larger and also increased with target speed (5.4, 8.0 and  
299  $12.0^\circ/\text{s}$  for the 10, 20 and 40°/s target, respectively). Figure 4C compares the average horizontal  
300 position/time landing between saccades toward the 20°/s target and saccades to the 10°/s (gray  
301 symbols) and 40°/s (black symbols) targets. The values with the 10°/s target were smaller than  
302 the values with the 20°/s target (gray symbols are situated below the diagonal line of equality)  
303 whereas the values with the 40°/s target were larger than those obtained with the 20°/s target  
304 (almost all black symbols above the diagonal line). Thus, within the same experiment, the size  
305 of the ipsipulsion was larger during saccades to the fastest target than during saccades to the  
306 slowest ones. Moreover, the injections which led to the larger horizontal errors with the 20°/s  
307 target were those caused the bigger changes with the other speeds. Statistically significant  
308 correlations were indeed found between the average horizontal position/time landing values  
309 calculated with the 20°/s and 10°/s targets (Bravais-Pearson correlation coefficient  $R = 0.94$ , P

310 < 0.05) as well as between the mean values obtained with the 20°/s and 40°/s targets ( $R(x,y) =$   
311 0.93,  $P < 0.05$ ).

312 **Figure 5 approximately here**

313 In our previous report, we documented the dysmetria of horizontal interceptive saccades  
314 after cFN inactivation: ipsilesional saccades are hypermetric whereas contralesional saccades  
315 are hypometric (Bourrelly et al. 2018a). Like the dysmetria that affects horizontal saccades  
316 toward a static target (Goffart et al. 2004, in preparation), the sizes of the ipsilesional and  
317 contralesional dysmetria are unrelated. However, it is known that the cFN projects to the region  
318 in the contralateral medullary reticular formation (medRF) where premotor inhibitory burst  
319 neurons (IBNs) are located (Noda et al. 1990) and that these neurons, in addition to firing a  
320 burst during horizontal saccades, also fire during vertical saccades (Scudder et al. 1988; van  
321 Gisbergen et al. 1981). Because of this involvement of IBNs in horizontal and vertical saccades,  
322 it is quite reasonable to consider that a common dysfunction causes the ipsipulsion of vertical  
323 saccades and the dysmetria of horizontal saccades (Goffart et al. 2004). Therefore, we tested  
324 the relation between these two disorders and found a significant correlation between the average  
325 horizontal position/time landings of ipsilesional horizontal saccades and vertical saccades  
326 toward the 10°/s ( $R = 0.77$ ,  $P < 0.05$ ), 20°/s ( $R = 0.62$ ,  $P < 0.05$ ) and 40°/s ( $R = 0.81$ ,  $P < 0.05$ )  
327 targets (Fig. 5A). When the correlation was instead tested between the horizontal position/time  
328 landings of contralesional horizontal saccades and vertical saccades, the coefficients were  
329 smaller and negative. Furthermore, the correlation did not reach statistical significance when  
330 the target moved at 10°/s ( $R = -0.41$ ,  $P > 0.05$ ) and 40°/s ( $R = -0.13$ ,  $P > 0.05$ ). A significant  
331 correlation was found only with the 20°/s target ( $R = -0.47$ ,  $P < 0.05$ ) (Fig. 5B). Then, for each  
332 experiment, we subtracted the average contralesional position/time landing from the  
333 ipsilesional position/time landing, the resulting difference (hereafter called net bilateral effect  
334 on horizontal saccades) characterizing the dysmetria of saccades made toward a target moving

335 horizontally (leftward or rightward). In this case, we found significant correlations between the  
336 horizontal position/time landings of vertical saccades and the net bilateral effect on horizontal  
337 saccades (Fig. 5C) that were stronger than those obtained with ipsilesional horizontal saccades  
338 ( $10^\circ/s$  target:  $R = 0.91$  versus  $0.77$ ;  $20^\circ/s$   $R = 0.81$  versus  $0.62$ ;  $40^\circ/s$ :  $R = 0.90$  versus  $0.81$ ).

339 In summary, after muscimol injection in the cFN, all vertical saccades made toward a  
340 target moving at a constant speed along the vertical meridian were deviated horizontally toward  
341 the injected side. Their vertical components were slightly affected but not as dramatically as  
342 the horizontal component. The size of the ipsipulsion differed between experiments and the  
343 average horizontal position/time landing increased with the target speed. Moreover, the  
344 ipsipulsion is correlated with the dysmetria that impaired the horizontal (ipsilesional and  
345 contralesional) saccades.

346 **Figure 6 approximately here**

347 In the figure 4C, we showed that the ipsipulsion of vertical saccades depends upon the  
348 target speed. To further explore this dependence, we tested saccades toward a target that moved  
349 with continuous acceleration or deceleration. If the ipsipulsion depends on target speed, the  
350 horizontal landing position should increase with later landing times when the target accelerates  
351 but decrease or stagnate when it decelerates. Figure 6 describes the horizontal landing position  
352 and time of saccades to a target moving with an increasing (top row) and decreasing speed  
353 (bottom row) for three experiments (A3: left column; Bi8: middle and Bi9: right). During the  
354 control sessions (open squares), the saccades landed on locations situated along the vertical  
355 meridian (open symbols are close to the line of zero horizontal position) whereas after muscimol  
356 injection (filled squares), they landed on locations which were shifted toward the injected side  
357 (see negative position values in experiments A3 and Bi8 and positive values in experiment Bi9).  
358 For these three experiments, the ipsipulsion of vertical saccades did not depend on the

359 instantaneous speed of the target. Statistically significant correlations were found in only two  
360 experiments: A6 (positive correlation  $R = 0.54$ , injection in the right cFN) and A2 (negative  
361 correlation  $R = -0.35$ , left cFN). For the other experiments, no correlation was found between  
362 the horizontal landing position and the landing time when the target accelerated ( $R$  values  
363 ranged from  $-0.25$  to  $0.19$ ,  $P$ -values  $> 0.05$ ). Concerning the saccades toward a decelerating  
364 target, no statistically significant correlation was found between the horizontal landing position  
365 and the landing time ( $R$  values ranged from  $-0.42$  to  $0.34$ ,  $P$ -values  $> 0.05$ ). In summary, we  
366 found no evidence suggesting that the ipsipulsion depends on the instantaneous target speed:  
367 the horizontal landing position neither increased with later landing times when the target  
368 accelerated nor decreased when it decelerated.

369 **Figure 7 approximately here**

370 Fig. 7 documents the mean values of vertical (A) and horizontal (B) position/time  
371 landing of saccades toward the accelerating (gray symbols) and decelerating (black symbols)  
372 targets, before and after muscimol injection, as a summary of our results. The vertical  
373 position/time landing of saccades was changed after muscimol injection, more with the  
374 decelerating target than with the accelerating one (Fig. 7A). With the accelerating target, the  
375 pre- and post-injection mean values of vertical position/time landing were not significantly  
376 different (Wilcoxon test,  $P = 0.47$ ) whereas with the decelerating target, the post-injection  
377 values were significantly different from pre-injection values (16% average increase,  $P < 0.05$ ).  
378 Regarding the horizontal position/time landing (Fig. 7B), it increased from  $0.1 \pm 0.7^\circ/s$  (range:  
379  $-0.8 - 1.9^\circ/s$ ) to  $5.0 \pm 2.9^\circ/s$  (range:  $0.8 - 9.5^\circ/s$ ) after muscimol injection with the accelerating  
380 target and from  $0.0 \pm 1.8^\circ/s$  (range:  $-3.6 - 3.4^\circ/s$ ) to  $11.6 \pm 5.9^\circ/s$  (range:  $2.6 - 20.1^\circ/s$ ) with the  
381 decelerating target. In both groups of saccades, the changes were statistically significant ( $P <$   
382  $0.05$ ). Like saccades toward a target moving with a constant speed, the mean values of  
383 horizontal landing position were also variable between the different muscimol injections (see

384 range values reported above and the scatter of post-lesion data points in Fig. 7B). Finally, the  
385 injections which led to the larger horizontal position/time landings with the 20°/s moving target  
386 were those which led to the bigger changes with the accelerating and decelerating targets (Fig.  
387 7C). Statistically significant correlations were indeed found between the horizontal  
388 position/time landings of saccades toward the 20°/s and those directed toward the accelerating  
389 (Bravais-Pearson correlation coefficient  $R(x,y) = 0.86$ ,  $P < 0.05$ ) or decelerating target ( $R(x,y)$   
390  $= 0.90$   $P < 0.05$ ). In summary, all vertical saccades toward a target moving with a changing  
391 speed were shifted horizontally after muscimol injection in the cFN. Like saccades toward a  
392 target moving at a constant speed, the amplitude of their vertical component was slightly  
393 increased after muscimol inactivation. Their horizontal component was biased toward the  
394 injected side with a magnitude which differed between experiments. The ipsipulsion was larger  
395 for saccades aimed toward a fast target than toward a slow target. It was also smaller when the  
396 target accelerated than when it decelerated.

397         As for saccades to a target moving horizontally, the larger deficit with fast targets can  
398 result from the fact that at identical landing times, a fast target is more eccentric than a slow  
399 one. The dependency of the ipsipulsion upon the target speed can result from the fact that a  
400 larger amplitude was required to intercept the target when it moves fast. Studies of vertical  
401 saccades toward a static target do indeed show that after cFN inactivation, the ipsipulsion  
402 increases with more eccentric targets (Goffart et al. 2004; Iwamoto and Yoshida 2002; Quinet  
403 and Goffart 2007). However, increasing target eccentricity enhances both the amplitude and  
404 duration of saccades for larger saccades that last longer. It is not known which of these  
405 parameters affect more the magnitude of ipsipulsion. Therefore, we tested the correlation  
406 between the horizontal landing position and saccade duration for each post-injection session.  
407 The parameters of the equations fitting the relation between the horizontal landing position and  
408 the saccade duration after muscimol injection are documented for all the experiments (upward

409 and downward movements pooled together) in table 1 (constant speeds) and table 2 (changing  
410 speeds). The correlation was statistically significant in 13 out of 44 test sessions (corresponding  
411 to 30% of cases) with coefficients of correlation ranging from 0.37 to 0.72. When we instead  
412 considered the relation between the horizontal landing position and vertical saccade amplitude,  
413 statistically significant correlations were found in 30 out of 44 sessions (corresponding to 68%  
414 of the post-injection sessions), with coefficients of correlation ranging from 0.38 to 0.81. The  
415 parameters of the equations fitting the relation between the horizontal landing position and the  
416 vertical saccade amplitude after muscimol injection are documented for all the experiments  
417 (upward and downward movements pooled together) in table 1 (target moving at a constant  
418 speed) and table 2 (accelerating and decelerating targets). In several instances, the correlation  
419 between the saccade duration and the horizontal landing position ( $R(\text{Dur},\text{HorP})$ ) did not reach  
420 statistical significance whereas the correlation between the saccade amplitude and the  
421 horizontal landing position ( $R(\text{Amp},\text{HorP})$ ) was statistically significant (see Table 1:  
422 experiments A3, A5, A6 and Bi9 for the 10°/s target; A2, A3, A6, Bi9 and Bi10 for the 20°/s  
423 target; in A3, A5 and Bi7 for the 40°/s target). Likewise, when we consider the saccades toward  
424 an accelerating target (leftmost columns in Table 2),  $R(\text{Dur},\text{HorP})$  was not statistically  
425 significant although  $R(\text{Amp},\text{HorP})$  was during the experiments A2 and A6. Finally, when the  
426 target was decelerating (rightmost columns in Table 2),  $R(\text{Dur},\text{HorP})$  was not statistically  
427 significant but  $R(\text{Amp},\text{HorP})$  was significant during the experiments A3, A6, Bi8 and Bi10.  
428 Considering all 44 sessions, a significant correlation  $R(\text{Dur},\text{HorP})$  without significant  
429 correlation  $R(\text{Amp},\text{HorP})$  was observed in one single experiment (Bi8, accelerating target).  
430 Altogether, these results strongly suggest that the ipsipulsion increased mostly because  
431 saccades had larger amplitudes than because they lasted longer.

432

**Figure 8 approximately here**

433 To illustrate this correlation between the vertical amplitude of saccades and the  
434 ipsipulsion, Fig. 8 plots the horizontal landing position as a function of vertical saccade  
435 amplitude before and after muscimol injection. Both upward and downward saccades were  
436 included (the amplitude of downward saccades was multiplied by -1). The relations are shown  
437 for four injections made in the left cFN of monkey A (experiments A2 and A3, top row) and Bi  
438 (experiments Bi7 and Bi8, bottom) for saccades to targets moving with a constant speed (light  
439 gray, dark gray and black symbols correspond to the 10, 20 and 40°/s target speeds,  
440 respectively). Negative values of horizontal eye position indicate that the saccades were  
441 deviated toward the left (inactivated side). Thus, we can see that while the target speed increases  
442 from 10 to 40°/s (symbols with different shades of grey), the horizontal landing position and  
443 the vertical saccade amplitude increased. During experiment A2 (Fig. 8A), as the target speed  
444 increased, the horizontal landing position changed from  $-0.3 \pm 0.3^\circ$  (10°/s) to  $-0.7 \pm 0.5^\circ$  (20°/s)  
445 and  $-1.4 \pm 0.8^\circ$  (40°/s), while the vertical amplitude increased from  $2.8 \pm 0.6^\circ$  (10°/s) to  $5.1 \pm$   
446  $1.1^\circ$  (20°/s) and  $10.2 \pm 1.9^\circ$  (40°/s). Likewise, during experiment A3 (Fig. 8B), the horizontal  
447 landing position increased from  $-0.3 \pm 0.3^\circ$  to  $-0.5 \pm 0.4^\circ$  and  $-1.3 \pm 0.6^\circ$  while the vertical  
448 amplitude increased from  $2.7 \pm 0.6^\circ$  to  $5.1 \pm 1.1^\circ$  and  $10.5 \pm 1.1^\circ$  (values for the 10, 20 and  
449 40°/s target speed, respectively). The same relationship was found in monkey Bi. During  
450 experiment Bi7 (Fig. 8C), the horizontal landing position increased from  $-2.4 \pm 0.7^\circ$  to  $-3.4 \pm$   
451  $1.6^\circ$  and  $-4.3 \pm 1.1^\circ$  and the vertical amplitude from  $2.2 \pm 0.7^\circ$  to  $5.1 \pm 1.2^\circ$  and  $9.0 \pm 1.3^\circ$ .  
452 Finally, during experiment Bi8 (Fig. 8D), the horizontal landing position increased from  $-2.0 \pm$   
453  $0.7^\circ$  (10°/s) to  $-2.8 \pm 0.8^\circ$  (20°/s) to  $-3.7 \pm 1.0^\circ$  (40°/s), while the vertical amplitude increased  
454 from  $2.2 \pm 0.6^\circ$  to  $5.0 \pm 1.6^\circ$  and  $9.1 \pm 1.1^\circ$ . A relation was observed between the horizontal  
455 landing position and the vertical amplitude of saccades. Each inset graph plotted in the right  
456 part of the panels of Figure 8 shows an overlap of data points corresponding to saccades to a  
457 target moving at constant speed (gray symbols) and to an accelerating or decelerating target

458 (black symbols). In summary, after cFN inactivation, the landing position of vertical saccades  
459 was deviated toward the injected side by an amount that varied between experiments and that  
460 was larger when the target moved quickly than when it moved slowly. The dependency of the  
461 ipsipulsion upon the target speed indicates that the saccade oculomotor system has access to  
462 different signals when the target moves at different speeds. However, the use of accelerating  
463 and decelerating target enabled us to exclude a dependency upon the instantaneous speed of the  
464 target. Further analyses revealed that the ipsipulsion was more frequently correlated with the  
465 vertical amplitude of saccades rather than with their duration.

466 **Discussion**

467 This study is the first to describe the consequences of unilateral pharmacological  
468 inactivation of cFN on the generation of vertical saccades toward a moving target. As for the  
469 saccades toward a static target, interceptive saccades exhibit a horizontal deviation of their  
470 trajectory toward the lesioned side (ipsipulsion; Figs. 3, 4B and 7B) whereas the vertical  
471 component is barely affected (Figs. 2, 3, 4A and 7A). The magnitude of the ipsipulsion is larger  
472 for fast targets than for slowly moving targets (Fig. 4C) but the use of accelerating and  
473 decelerating targets indicates that this relation is due less to the instantaneous target speed (Fig.  
474 6) than to the saccade size. Indeed, like saccades toward a static target, the ipsipulsion increased  
475 with the vertical amplitude of saccades (Fig. 8). Statistical analyses made across all sessions  
476 indicate that the correlations between the ipsipulsion and the vertical amplitude were more  
477 frequent than the correlations between the ipsipulsion and the duration. Moreover, in several  
478 sessions, the correlation between the ipsipulsion and the duration of saccades did not reach  
479 statistical significance whereas the correlation with the vertical amplitude was significant  
480 (Tables 1 and 2). Below, we explain the neurophysiological mechanisms leading to the  
481 ipsipulsion of vertical saccades and further develop facts which call for an alternative approach  
482 to investigate the neurophysiology of visually-guided eye movements and their cerebellar  
483 control.

484 **Figure 9 approximately here**

485 ***How does bilateral fastigial activity influence the trajectory of saccades?***

486 Numerous works show that the activity of cFN neurons plays a crucial role in the  
487 cerebellar control of saccade generation. Two major reasons led us to investigate their influence  
488 on the trajectory of saccades toward a target moving along the vertical meridian: 1) vertical  
489 saccades are deviated horizontally after unilateral cFN inactivation and 2) the same etiology  
490 can account for this ipsipulsion and the dysmetria of horizontal saccades. In the framework of

491 negative feedback control in which an internal estimate of current eye position (or  
492 displacement) is compared to a desired eye position (or displacement) command (Robinson  
493 1975; Sparks 1989; Becker 1995; Pola 2002), a horizontal bias could impair vertical saccades  
494 in a cumulative manner as long as motor error is not zeroed and omnipause neurons do not  
495 resume their activity. Our results do not support this link between the horizontal targeting error  
496 and the duration of vertical saccades because the magnitude of the ipsipulsion was less  
497 frequently dependent upon the duration than the amplitude, and because in many cases, the  
498 correlation between the ipsipulsion and the duration did not reach statistical significance  
499 whereas the correlation between the ipsipulsion and the amplitude was statistically significant.  
500 An independence between the dysmetria and duration of gaze shifts was already noticed in the  
501 head unrestrained cat after cFN inactivation (see Figs. 5 and 6 in Goffart et al. 1998). Finally,  
502 it is worth reminding that neither Kaneko (1996) nor Soetedjo et al. (2000) reported changes in  
503 the accuracy of saccades when the nucleus raphe interpositus is lesioned or inactivated. The  
504 dysmetria of saccades after cFN inactivation is therefore not caused (but permitted) by the pause  
505 of OPNs (under the influence of the vertical burst generator). We propose that the ipsipulsion  
506 is driven by action potentials that abducens neurons emit under the influence of unbalanced  
507 input from excitatory and inhibitory burst neurons.

508         The known physiology of the saccade-related circuitry indeed explains the ipsipulsion  
509 of vertical saccades: if the activity of neurons in the left and right abducens nuclei is not  
510 balanced during vertical saccades, there will be horizontal deviation of the eyes. The elevated  
511 speed and the large magnitude of the ipsipulsion during head-unrestrained gaze shifts (Quinet  
512 and Goffart 2007) indicate that this imbalance is not caused by a reduced inhibition that IBNs  
513 in the contralateral medullary reticular formation exert upon neurons in the abducens nucleus  
514 ipsilateral to the inactivated cFN (synapses a and b in Fig. 9). An excitatory drive is required  
515 and we hypothesize that it is conveyed by neurons in the opposite (unaffected) cFN (synapse

516 f). Transmitted by crossed projections (Noda et al. 1990), their spikes excite premotor burst  
517 neurons in the pontomedullary reticular formation ipsilateral to the inactivated cFN, which in  
518 turn activate motor and internuclear neurons in the ipsilateral abducens nucleus (synapses g and  
519 h). This crossed excitatory influence upon premotor burst neurons is supported by the fact that  
520 fastigial electrical stimulation evokes contralateral saccades (Cogdell et al. 1977; Noda et al.  
521 1988; Quinet and Goffart 2015). It is also consistent with the contrapulsion of vertical saccades  
522 when the oculomotor vermis is asymmetrically lesioned (Takagi et al. 1998) or inactivated with  
523 muscimol (Nitta et al. 2007). This crossed fastigioreticular projection does not concern the  
524 reticulospinal neurons that Takahashi et al. (2014) identified in the cat. Indeed, if it also exists  
525 in the macaque, this fastigio-reticulospinal connection is likely involved in the postural tone of  
526 the head because the head barely moves when the cFN is electrically stimulated (Quinet and  
527 Goffart 2009). Also, during cFN inactivation in both the cat and monkey, the head exhibits an  
528 ipsilesional deviation (Goffart and Péliesson 1998; Quinet and Goffart 2005). Furthermore, the  
529 increase of ipsipulsion with saccade amplitude indicates that abducens neurons and excitatory  
530 burst neurons (EBNs) fire more as the vertical amplitude increases. Although EBNs do not  
531 normally fire during vertical saccades (Strassman et al. 1986a; Sparks et al. 2002) and unilateral  
532 inactivation of their territory yields no ipsipulsion (Barton et al. 2003), it is possible that after  
533 cFN inactivation, ipsilateral MNs, INs and EBNs abnormally fire during vertical saccades  
534 because they are released from the inhibition exerted by burst neurons (IBNs) in the  
535 contralateral reticular formation (synapses a, b and d; Cullen and Guitton 1997; Scudder et al.  
536 1988; Strassman et al. 1986b). Those IBNs are silenced because of the suppression of their  
537 fastigial drive (synapse i) by the muscimol injection, because also of the inhibition exerted by  
538 IBNs located in the opposite side (synapse j) and recruited by neurons in the unaffected cFN  
539 (synapse e). Scudder et al. (1988) indeed showed that IBNs fire more spikes as the size of  
540 vertical saccades increases (see also van Gisbergen et al. 1981). Thus, released from the

541 inhibitory influence of contralateral IBNs (synapses a and b), MNs and INs emit spikes that  
542 deviate vertical saccades with a magnitude that increases with saccade size. The burst would be  
543 triggered by excitatory input from EBNs or from other neurons innervating the abducens  
544 nucleus (Langer et al. 1986; Ugolini et al. 2006).

545         According to the bilateral hypothesis, the activity of saccade-related fastigial neurons  
546 influences the horizontal component of all saccades (vertical and/or horizontal). Ipsilesional  
547 saccades overshoot horizontally their target because following cFN inactivation, the agonist  
548 motor neurons receive a drive from excitatory burst neurons (synapses g and h in Fig. 9) that  
549 exceeds the pre-lesional drive, as it is no longer attenuated by spikes emitted by IBNs in the  
550 contralateral side (synapses a, b and d). Indeed, these IBNs not only lack their fastigial  
551 excitatory input (synapse i) but they are also inhibited by IBNs driven by neurons in the  
552 unaffected cFN (synapse e). Likewise, contralesional saccades prematurely stop for two  
553 reasons: because the agonist motor neurons lack the drive they usually receive from EBNs (as  
554 a result of suppressing their fastigial input; synapse k) and because the opposite (unaffected)  
555 cFN excites IBNs which in turn inhibit the agonist motor neurons (synapses l and m). Thus,  
556 regardless of saccade direction, the same bilateral mechanism (i.e., an altered balance of  
557 excitatory and inhibitory input to the motor neurons) explains the effects on the horizontal  
558 component of all saccades. This conclusion is further supported when the results from the  
559 present study are synthesized with those reported in Bourrelly et al. (2018a). Indeed, the net  
560 bilateral effect of inactivation on horizontal saccades (calculated by subtracting the average  
561 contralesional position/time landing ratio from the ipsilesional ratio) is strongly correlated with  
562 the horizontal position/time landing of vertical saccades.

563

564 *Recasting the neurophysiology of saccades*

565 In the preceding section as well as in our previous reports (Bourrelly et al. 2018a,b;  
566 Goffart et al. 2004; Guerrasio et al. 2010; Quinet & Goffart 2007), the oculomotor disorders  
567 observed after cFN inactivation were explained without assuming perturbations of some  
568 internal (and putative) estimate of the eye kinematics, as one might expect for example, if their  
569 input from Purkinje cells in the oculomotor vermis were to encode the instantaneous velocity  
570 of saccades (Herzfeld et al. 2015). In this section, we want to further develop additional  
571 concerns which support our alternative viewpoint and call for recasting the neurophysiology of  
572 eye movements (Goffart et al. 2018; Goffart 2019).

573 First of all, it is important to realize that if the recording of eye muscle tension had been  
574 used more frequently (Davis-Lopez de Carrizosa et al., 2011; Gamlin and Miller; 2012;  
575 Lennerstrand et al. 1993; Miller and Robins 1992) than the recording the orientation of the eyes  
576 during neurophysiological experiments, different processes and models might have been  
577 proposed. Then, it is also important to consider the fact that the time course of saccades is not  
578 exclusively determined by the discharge of premotor and motor neurons. It involves changes in  
579 the firing rate of neurons distributed in many brain regions such as the frontal cortex (Dias and  
580 Segraves 1999), the mesencephalon (Aizawa and Wurtz 1998; Sparks et al. 1990), the pons  
581 (Kaneko and Fuchs 2006), the medio-posterior cerebellum (Goffart et al. 2003; Kojima et al.  
582 2010) and the reticular formation (Barton et al. 2003; Soetedjo et al. 2000). Right upstream  
583 from the extraocular muscle fibers, saccades are engendered by an abrupt increase in the firing  
584 rate of motor neurons which innervate the agonist muscles and a concomitant decrease in the  
585 discharge of neurons innervating the antagonist muscles. Due to the highly damped nature of  
586 the oculomotor plant (Robinson 1964), a braking action is not exerted upon antagonist motor  
587 neurons to stop the saccade (Robinson 1970; Schiller 1970). Thus, the agonist burst duration  
588 increases with the duration of saccades and determines their size and the saturated firing rate  
589 leads to a discharge frequency which is poorly related to saccade speed (Fuchs and Luschei

590 1970; Robinson 1970; Schiller 1970; Sparks and Hu 2006). Synchronous presynaptic spikes  
591 converging upon the motor neurons could be one way to overcome the limitations of interspike  
592 intervals (Schiller 1970; Goffart et al. 2017a). For the generation of horizontal saccades, the  
593 burst causing the phasic contraction of the medial rectus (and the saccade of the contralateral  
594 eye) originates in burst-tonic (internuclear) neurons in the abducens nucleus while the burst  
595 causing the phasic contraction of the lateral rectus (saccade of the ipsilateral eye) originates in  
596 abducens motoneurons. These bursts are caused by excitatory burst neurons in the paramedian  
597 pontine reticular formation (Keller 1974; Luschei and Fuchs 1972; Strassman et al. 1986a).

598         In several synthesis articles, we can read that the discharge profile of burst neurons is a  
599 “replica of eye velocity” (Scudder et al. 2002) and that pontine and midbrain EBNs encode  
600 saccade velocity by the frequency of spikes (Sparks 2002). Their instantaneous firing rate would  
601 be closely related with instantaneous eye velocity (Leigh and Zee 2006, page 126), as supported  
602 by several recording studies in the premotor and motor neurons (e.g., Cromer and Waitzman  
603 2007; Cullen and Guitton 1997; King and Fuchs 1979; Sylvestre and Cullen 1999). For several  
604 years, kinematic notions were used to interpret the spiking activity of neurons and to model the  
605 generation of saccades. Yet, when we examine the firing rate of premotor neurons, we discover  
606 that they do not exhibit the same time course as instantaneous eye velocity (see Figs. 2 and 3 in  
607 Hu et al. 2007, Fig. 3C in Sparks and Hu 2006 and Fig. 5 in van Gisbergen et al. 1981). In fact,  
608 the meticulous inspection reveals that the instantaneous discharge of burst neurons is almost  
609 clock-like and quasi-regular (Hu et al. 2007), radically different from the bell-shaped profile  
610 shown by studies which convolve each spike with a Gaussian kernel.

611         The relation between the firing rate and the instantaneous saccade velocity was recently  
612 extended to more central neurons in the superior colliculus (Smalianchuk et al. 2018) and the  
613 oculomotor vermis (Herzfeld et al. 2015). In agreement with the crucial role of these two  
614 regions in continuously driving the saccades (Goffart et al. 2003; Goossens and van Opstal

615 2006), these studies proposed that the discharge of their neurons encodes the instantaneous  
616 velocity. Two major observations must, nevertheless, be considered. Firstly, a model factoring  
617 muscle tension and its first derivative fits better the instantaneous firing rate of motoneurons  
618 than a model that uses eye position, velocity and acceleration (Davis-Lopez de Carrizosa et al.,  
619 2011). The putative velocity commands must therefore be translated into force-related  
620 commands somewhere before reaching the motor neurons. Interposed between the saccade-  
621 related bursts of Purkinje cells and the premotor burst neurons, the caudal fastigial nuclei host  
622 a population of neurons which emit spikes that have a strong impact on the time course of  
623 saccades toward their landing position. Changes in cFN activity alter not only the endpoint of  
624 saccades (Goffart et al. 2003; Noda et al. 1991) but also their trajectory (see Figs. 1 and 7 in  
625 Goffart et al. 2004; Fig. 1 in Iwamoto and Yoshida 2002). However, the absence of relation  
626 between their firing rate and saccade velocity (Fuchs et al. 1993; Helmchen et al. 1994; Ohtsuka  
627 and Noda 1991) draws into question the suggestion that the population discharge of Purkinje  
628 cells “encodes” instantaneous saccade velocity (Herzfeld et al. 2015). When correlations are  
629 found between the population firing rate and saccade velocity, caution must be taken that they  
630 do not result from idiosyncratic (all monkeys do not make the same saccade amplitude with the  
631 same speed) or unspecific factors like different levels of motivation or arousal (Fuchs et al.  
632 1993) as shown also in the deep superior colliculus (Ikeda and Hikosaka 2007; Soetedjo et al.  
633 2000).

634

### 635 ***Conclusion***

636         Instead of reflecting the reduction of an internal signal encoding the horizontal distance  
637 between gaze and target positions (or displacements), we propose that the horizontal component  
638 of saccades is the outcome of a process which restores, under bilateral fastigial control, an  
639 equilibrium (symmetry) that has been broken by asymmetric descending input (from cortical

640 eye fields and deep superior colliculus) to the horizontal saccade generators (Goffart et al. 2018;  
641 Goffart 2019). In the future, more studies will have to clarify the cerebellar control of the  
642 vertical component of saccades (Quinet and Goffart 2015; Robinson 2000) and its coupling  
643 with the processes controlling their horizontal component (Goffart et al. 2005).

644

645 **References**

- 646 Aizawa H, Wurtz RH. Reversible inactivation of monkey superior colliculus. I. Curvature of  
647 saccadic trajectory. *J Neurophysiol* 79: 2082-2096, 1998. doi: [10.1152/jn.1998.79.4.2082](https://doi.org/10.1152/jn.1998.79.4.2082)
- 648 Barton EJ, Nelson JS, Gandhi NJ, Sparks DL. Effects of partial lidocaine inactivation of the  
649 paramedian pontine reticular formation on saccades of macaques. *J Neurophysiol* 90: 372-  
650 386, 2003. doi: [10.1152/jn.01041.2002](https://doi.org/10.1152/jn.01041.2002)
- 651 Becker W. Models of oculomotor function: An appraisal of the engineer's intrusion into  
652 oculomotor physiology. *Studies Vis Inform Processing* 6: 23-46, 1995.
- 653 Bourrelly C, Quinet J, Cavanagh P, Goffart L. Learning the trajectory of a moving visual  
654 target and evolution of its tracking in the monkey. *J Neurophysiol* 116: 2739–2751, 2016. doi:  
655 [10.1152/jn.00519.2016](https://doi.org/10.1152/jn.00519.2016)
- 656 Bourrelly C, Quinet J, Goffart L. The caudal fastigial nucleus and the steering of saccades  
657 toward a moving visual target. *J Neurophysiol* 120: 421–438, 2018a. doi:  
658 [10.1152/jn.00141.2018](https://doi.org/10.1152/jn.00141.2018)
- 659 Bourrelly C, Quinet J, Goffart L. Pursuit disorder and saccade dysmetria after caudal fastigial  
660 inactivation in the monkey. *J Neurophysiol* 120: 1640-1654, 2018b. doi:  
661 [10.1152/jn.00278.2018](https://doi.org/10.1152/jn.00278.2018)
- 662 Bourrelly C, Quinet J, Goffart L. Unsupervised dynamic morphing of a spatiotemporal visual  
663 event during its oculomotor tracking. *J Vision* 14: 492, 2014.
- 664 Buzunov E, Mueller A, Straube A, Robinson FR. When during horizontal saccades in monkey  
665 does cerebellar output affect movement? *Brain Res* 1503: 33-42, 2013. doi:  
666 [10.1016/j.brainres.2013.02.001](https://doi.org/10.1016/j.brainres.2013.02.001)
- 667 Cogdell B, Hassul M, Kimm J. Fastigial evoked eye movement and brain stem neuronal  
668 behavior in the alert monkey. *Arch Otolaryngol* 103: 658-666, 1977. doi:  
669 [10.1001/archotol.1977.00780280058008](https://doi.org/10.1001/archotol.1977.00780280058008)
- 670 Cromer JA, Waitzman DM. Comparison of saccade-associated neuronal activity in the  
671 primate central mesencephalic and paramedian pontine reticular formations. *J Neurophysiol*  
672 98: 835-850, 2007. doi: [10.1152/jn.00308.2007](https://doi.org/10.1152/jn.00308.2007)

673 Cullen KE, Guitton D. Analysis of primate IBN spike trains using system identification  
674 techniques. I. Relationship to eye movement dynamics during head-fixed saccades. J  
675 Neurophysiol 78: 3259-3282, 1997. doi : [10.1152/jn.1997.78.6.3259](https://doi.org/10.1152/jn.1997.78.6.3259)

676 Davis-López de Carrizosa MA, Morado-Díaz CJ, Miller JM, de la Cruz RR, Pastor ÁM. Dual  
677 encoding of muscle tension and eye position by abducens motoneurons. J Neurosci 31: 2271-  
678 2279, 2011. doi: [10.1523/JNEUROSCI.5416-10.2011](https://doi.org/10.1523/JNEUROSCI.5416-10.2011)

679 Dias EC, Segraves MA. Muscimol-induced inactivation of monkey frontal eye field: effects  
680 on visually and memory-guided saccades. J Neurophysiol 81: 2191-2214, 1999. doi:  
681 [10.1152/jn.1999.81.5.2191](https://doi.org/10.1152/jn.1999.81.5.2191)

682 Fuchs AF, Brettler S, Ling L. Head-free gaze shifts provide further insights into the role of the  
683 medial cerebellum in the control of primate saccadic eye movements. J Neurophysiol 103:  
684 2158–2173, 2010. doi: [10.1152/jn.91361.2008](https://doi.org/10.1152/jn.91361.2008)

685 Fuchs AF, Luschei ES. Firing patterns of abducens neurons of alert monkeys in relationship  
686 to horizontal eye movement. J Neurophysiol 33: 382–392, 1970. doi:  
687 [10.1152/jn.1970.33.3.382](https://doi.org/10.1152/jn.1970.33.3.382)

688 Fuchs AF, Kaneko CRS, Scudder CA. Brainstem control of saccadic eye movements. Ann  
689 Rev Neurosci 8: 307-337, 1985. doi: [10.1146/annurev.ne.08.030185.001515](https://doi.org/10.1146/annurev.ne.08.030185.001515)

690 Fuchs AF, Robinson FR, Straube A. Role of the caudal fastigial nucleus in saccade  
691 generation. I. Neuronal discharge pattern. J Neurophysiol 70: 1723-1740, 1993. doi:  
692 [10.1152/jn.1993.70.5.1723](https://doi.org/10.1152/jn.1993.70.5.1723)

693 Gamlin, PD, Miller JM. Extraocular muscle motor units characterized by spike-triggered  
694 averaging in alert monkey. J Neurosci Methods 204: 159-167, 2012. doi:  
695 [10.1016/j.jneumeth.2011.11.012](https://doi.org/10.1016/j.jneumeth.2011.11.012)

696 Goffart L. Kinematics and the neurophysiological study of visually-guided eye movements.  
697 Prog Brain Res 249:375-384, 2019. doi: [10.1016/bs.pbr.2019.03.027](https://doi.org/10.1016/bs.pbr.2019.03.027)

698 Goffart L, Bourrelly C, Quinet J. Synchronizing the tracking eye movements with the motion  
699 of a visual target: Basic neural processes. Prog Brain Res;236: 243-268, 2017a. doi:  
700 [10.1016/bs.pbr.2017.07.009](https://doi.org/10.1016/bs.pbr.2017.07.009)

701 Goffart L, Bourrelly C, Quinton JC. Neurophysiology of visually-guided eye movements:  
702 Critical review and alternative viewpoint. *J Neurophysiol* 120: 3234-3245, 2018. doi:  
703 [10.1152/jn.00402.2018](https://doi.org/10.1152/jn.00402.2018)

704 Goffart L, Chen LL, Sparks DL. Saccade dysmetria during functional perturbation of the  
705 caudal fastigial nucleus in the monkey. *Ann NY Acad Sci* 1004: 220-228, 2003. doi:  
706 [10.1196/annals.1303.019](https://doi.org/10.1196/annals.1303.019)

707 Goffart L, Chen LL, Sparks DL. Deficits in saccades and fixation during muscimol  
708 inactivation of the caudal fastigial nucleus in the rhesus monkey. *J Neurophysiol* 92: 3351-  
709 3367, 2004. doi: [10.1152/jn.01199.2003](https://doi.org/10.1152/jn.01199.2003)

710 Goffart L, Koene A, Quinet J. Coupling between horizontal and vertical saccade generators  
711 after muscimol injection in the monkey caudal fastigial nucleus. *Soc Neurosci Abstr* 475.2,  
712 2005.

713 Goffart L, Pélisson D. Orienting gaze shifts during muscimol inactivation of caudal fastigial  
714 nucleus in the cat. I. Gaze dysmetria. *J Neurophysiol* 79: 1942–1958, 1998.  
715 doi:10.1152/jn.1998.79.4.1942

716 Goffart L, Pélisson D, Guillaume A. Orienting gaze shifts during muscimol inactivation of  
717 caudal fastigial nucleus in the cat. II. Dynamics and eye-head coupling. *J Neurophysiol* 79:  
718 1959-1976, 1998. doi: [10.1152/jn.1998.79.4.1959](https://doi.org/10.1152/jn.1998.79.4.1959)

719 Goffart L, Quinet J, Bourrelly C. Cerebellar control of saccades by the size of the active  
720 population in the caudal fastigial nucleus. S-5042-SfN, 2017b.

721 Goossens HH, Van Opstal AJ. Dynamic ensemble coding of saccades in the monkey superior  
722 colliculus. *J Neurophysiol* 95: 2326–2341, 2006. doi: [10.1152/jn.00889.2005](https://doi.org/10.1152/jn.00889.2005)

723 Guerrasio L, Quinet J, Büttner U, Goffart L. Fastigial oculomotor region and the control of  
724 foveation during fixation. *J Neurophysiol* 103: 1988-2001, 2010. doi: [10.1152/jn.00771.2009](https://doi.org/10.1152/jn.00771.2009)

725 Helmchen C, Straube A, Büttner U. Saccade-related activity in the fastigial oculomotor region  
726 of the macaque monkey during spontaneous eye movements in light and darkness. *Exp Brain*  
727 *Res* 98: 474–482, 1994. doi: [10.1007/BF00233984](https://doi.org/10.1007/BF00233984)

728 Hepp K, Henn V, Vilis T, Cohen B. Brainstem regions related to saccade generation. In: The  
729 neurobiology of saccadic eye movements. RH Wurtz and ME Goldberg (eds), Elsevier, 1989,  
730 pp 105-212.

731 Herzfeld DJ, Kojima Y, Soetedjo T, Shadmehr R. Encoding of action by the Purkinje cells of  
732 the cerebellum. *Nature* 526: 439-442, 2015. doi: [10.1038/nature15693](https://doi.org/10.1038/nature15693)

733 Horn AK. The reticular formation. *Progr Brain Res* 151: 127-155, 2006. doi:

734 Hu X, Jiang H, Gu C, Li C, Sparks DL. Reliability of oculomotor command signals carried by  
735 individual neurons. *Proc Nat Acad Sci* 104: 8137-8142, 2007. doi: [10.1073/pnas.0702799104](https://doi.org/10.1073/pnas.0702799104)

736 Ikeda T, Hikosaka O. Positive and negative modulation of motor response in primate superior  
737 colliculus by reward expectation. *J Neurophysiol* 98: 3163-3170, 2007. doi:  
738 [10.1152/jn.00975.2007](https://doi.org/10.1152/jn.00975.2007)

739 Iwamoto Y, Yoshida K. Saccadic dysmetria following inactivation of the primate fastigial  
740 oculomotor region. *Neurosci Lett* 325: 211-215, 2002. doi: [10.1016/s0304-3940\(02\)00268-9](https://doi.org/10.1016/s0304-3940(02)00268-9)

741 Kaneko CR. Effect of ibotenic acid lesions of the omnipause neurons on saccadic eye  
742 movements in rhesus macaques. *J Neurophysiol* 75: 2229-2242, 1996. doi:  
743 [10.1152/jn.1996.75.6.2229](https://doi.org/10.1152/jn.1996.75.6.2229)

744 Kaneko CR, Fuchs AF. Effect of pharmacological inactivation of nucleus reticularis tegmenti  
745 pontis on saccadic eye movements in the monkey. *J Neurophysiol* 95: 3698-3711, 2006. doi:  
746 [10.1152/jn.01292.2005](https://doi.org/10.1152/jn.01292.2005)

747 Keller EL. Participation of medial pontine reticular formation in eye movement generation in  
748 monkey. *J Neurophysiol* 37: 316-332, 1974. doi: [10.1152/jn.1974.37.2.316](https://doi.org/10.1152/jn.1974.37.2.316)

749 King WM, Fuchs AF. Reticular control of vertical saccadic eye movements by mesencephalic  
750 burst neurons. *J Neurophysiol* 42: 861-876, 1979. doi: [10.1152/jn.1979.42.3.861](https://doi.org/10.1152/jn.1979.42.3.861)

751 Kleine JF, Guan Y, Büttner U. Saccade-related neurons in the primate fastigial nucleus: what  
752 do they encode? *J Neurophysiol* 90: 3137-3154, 2003. doi: [10.1152/jn.00021.2003](https://doi.org/10.1152/jn.00021.2003)

753 Kojima Y, Soetedjo R, Fuchs AF. Effects of GABA agonist and antagonist injections into the  
754 oculomotor vermis on horizontal saccades. *Brain Res* 1366: 93-100, 2010. doi:  
755 [10.1016/j.brainres.2010.10.027](https://doi.org/10.1016/j.brainres.2010.10.027)

756 Langer T, Kaneko CR, Scudder CA, Fuchs AF. Afferents to the abducens nucleus in the  
757 monkey and cat. *J Comp Neurol* 245: 379-400, 1986. doi : [10.1002/cne.902450307](https://doi.org/10.1002/cne.902450307)

758 Leigh RJ, Zee DS. *The neurology of eye movements*. Oxford University Press, 2006.

759 Lennerstrand G, Tian S, Zhao TX. Force development and velocity of human saccadic eye  
760 movements. I: Abduction and adduction. *Clinical vision sciences* 8: 295-305, 1993.

761 Luschei ES, Fuchs AF. Activity of brain stem neurons during eye movements of alert  
762 monkeys. *J Neurophysiol* 35: 445-461, 1972. doi: [10.1152/jn.1972.35.4.445](https://doi.org/10.1152/jn.1972.35.4.445)

763 Miller JM, Robins D. Extraocular muscle forces in alert monkey. *Vision Res* 32: 1099-1113,  
764 1992. doi: [10.1016/0042-6989\(92\)90010-g](https://doi.org/10.1016/0042-6989(92)90010-g)

765 Moschovakis AK, Scudder CA, Highstein SM. The microscopic anatomy and physiology of  
766 the mammalian saccadic system. *Prog Neurobiol* 50: 133-254, 1996. doi: [10.1016/s0301-  
767 0082\(96\)00034-2](https://doi.org/10.1016/s0301-0082(96)00034-2)

768 Nitta T, Akao T, Kurkin S, Fukushima K. Involvement of the cerebellar dorsal vermis in  
769 vergence eye movements in monkeys. *Cereb Cortex* 18: 1042-1057, 2008. doi:  
770 [10.1093/cercor/bhm143](https://doi.org/10.1093/cercor/bhm143)

771 Noda H, Murakami S, Warabi T. Effects of fastigial stimulation upon visually-directed  
772 saccades in macaque monkeys. *Neurosci Res* 10(3):188-99, 1991. doi: [10.1016/0168-  
773 0102\(91\)90056-5](https://doi.org/10.1016/0168-0102(91)90056-5)

774 Noda H, Murakami S, Yamada J, Tamada J, Tamaki Y, Aso T. Saccadic eye movements  
775 evoked by microstimulation of the fastigial nucleus of macaque monkeys. *J Neurophysiol* 60:  
776 1036–1052, 1988. doi: [10.1152/jn.1988.60.3.1036](https://doi.org/10.1152/jn.1988.60.3.1036)

777 Noda H, Sugita S, Ikeda Y. Afferent and efferent connections of the oculomotor region of the  
778 fastigial nucleus in the macaque monkey. *J Comp Neurol* 302: 330-348, 1990. doi:  
779 [10.1002/cne.903020211](https://doi.org/10.1002/cne.903020211)

780 Ohtsuka K, Noda H. Saccadic burst neurons in the oculomotor region of the fastigial nucleus  
781 of macaque monkeys. J Neurophysiol 65: 1422-1434, 1991. doi: [10.1152/jn.1991.65.6.1422](https://doi.org/10.1152/jn.1991.65.6.1422)

782 Optican LM. Sensorimotor transformation for visually guided saccades. Ann NY Acad Sci  
783 1039: 132-148, 2005. doi: [10.1196/annals.1325.013](https://doi.org/10.1196/annals.1325.013)

784 Pola J. Models of the saccadic and smooth pursuit systems. In Models of the visual system, G.  
785 K. Hung et al. (eds.), Springer, Boston, MA, 2002, pp. 385-429.

786 Quinet J, Goffart L. Saccade dysmetria in head unrestrained gaze shifts after muscimol  
787 inactivation of the caudal fastigial nucleus in the monkey. J Neurophysiol 93: 2343–2349,  
788 2005. doi: [10.1152/jn.00705.2004](https://doi.org/10.1152/jn.00705.2004)

789 Quinet J, Goffart L. Head unrestrained gaze shifts after muscimol injection in the caudal  
790 fastigial nucleus of the monkey. J Neurophysiol 98: 3269-3283, 2007. doi:  
791 [10.1152/jn.00741.2007](https://doi.org/10.1152/jn.00741.2007)

792 Quinet J, Goffart L. Electrical microstimulation of the fastigial oculomotor region in the head-  
793 unrestrained monkey. J Neurophysiol 102: 320-336, 2009. doi: [10.1152/jn.90716.2008](https://doi.org/10.1152/jn.90716.2008)

794 Quinet J, Goffart L. Does the brain extrapolate the position of a transient moving target? J  
795 Neurosci 35: 11780-11790, 2015a. doi: [10.1523/JNEUROSCI.1212-15.2015](https://doi.org/10.1523/JNEUROSCI.1212-15.2015)

796 Quinet J, Goffart L. Cerebellar control of saccade dynamics: contribution of the fastigial  
797 oculomotor region. J Neurophysiol 113: 3323–3336, 2015b. doi: [10.1152/jn.01021.2014](https://doi.org/10.1152/jn.01021.2014)

798 Quinet J, Goffart L. Bilateral fastigial control of the horizontal amplitude of saccades:  
799 evidence from studying the orthogonal component after unilateral inactivation. Soc Neurosci  
800 Abstr 55.03, 2016.

801 Robinson DA. The mechanics of human saccadic eye movement. J Physiol 174: 245-264,  
802 1964. doi: [10.1113/jphysiol.1964.sp007485](https://doi.org/10.1113/jphysiol.1964.sp007485)

803 Robinson DA. Oculomotor unit behavior in the monkey. J Neurophysiol 33: 393-403,1970.  
804 doi: [10.1152/jn.1970.33.3.393](https://doi.org/10.1152/jn.1970.33.3.393)

805 Robinson DA. A quantitative analysis of extraocular muscle cooperation and squint.  
806 Investigative Ophthalmology & Visual Sci. 14: 801-825, 1975.

807 Robinson FR. Role of the cerebellar posterior interpositus nucleus in saccades I. Effect of  
808 temporary lesions. J Neurophysiol 84: 1289-1302, 2000. doi: [10.1152/jn.2000.84.3.1289](https://doi.org/10.1152/jn.2000.84.3.1289)

809 Robinson FR, Fuchs AF. The role of the cerebellum in voluntary eye movements. Annu Rev  
810 Neurosci 24: 981-1004, 2001. doi: [10.1146/annurev.neuro.24.1.981](https://doi.org/10.1146/annurev.neuro.24.1.981)

811 Robinson FR, Straube A, Fuchs AF. Role of the caudal fastigial nucleus in saccade  
812 generation. II. Effects of muscimol inactivation. J Neurophysiol 70: 1741–1758, 1993. doi:  
813 [10.1152/jn.1993.70.5.1741](https://doi.org/10.1152/jn.1993.70.5.1741)

814 Schiller PH. The discharge characteristics of single units in the oculomotor and abducens  
815 nuclei of the unanesthetized monkey. Exp Brain Res 10: 347-362, 1970. doi:  
816 [10.1007/BF02324764](https://doi.org/10.1007/BF02324764)

817 Scudder CA, Fuchs AF, Langer TP. Characteristics and functional identification of saccadic  
818 inhibitory burst neurons. J Neurophysiol 59: 1430-1454, 1988. doi:  
819 [10.1152/jn.1988.59.5.1430](https://doi.org/10.1152/jn.1988.59.5.1430)

820 Scudder CA, Kaneko CS, Fuchs AF. The brainstem burst generator for saccadic eye  
821 movements: a modern synthesis. Exp Brain Res 142: 439-462, 2002. doi: [10.1007/s00221-](https://doi.org/10.1007/s00221-001-0912-9)  
822 [001-0912-9](https://doi.org/10.1007/s00221-001-0912-9)

823 Smalianchuk I, Jagadisan UK, Gandhi NJ. Instantaneous midbrain control of saccade velocity.  
824 J. Neurosci. 38: 10156-10167, 2018. doi: [10.1523/JNEUROSCI.0962-18.2018](https://doi.org/10.1523/JNEUROSCI.0962-18.2018)

825 Soetedjo R, Kaneko CR, Fuchs AF. Evidence that the superior colliculus participates in the  
826 feedback control of saccadic eye movements. J Neurophysiol 87: 679–695, 2000. doi:  
827 [10.1152/jn.00886.2000](https://doi.org/10.1152/jn.00886.2000)

828 Sparks DL. The neural encoding of the location of targets for saccadic eye movements. J Exp  
829 Biol 146: 195-207, 1989. doi:

830 Sparks DL. The brainstem control of saccadic eye movements. Nat Rev Neurosci 3: 952-964,  
831 2002. doi: [10.1038/nrn986](https://doi.org/10.1038/nrn986)

832 Sparks DL, Barton EJ. Neural control of saccadic eye movements. *Curr Opin Neurobiol* 3:  
833 966–972, 1993. doi: [10.1016/0959-4388\(93\)90169-y](https://doi.org/10.1016/0959-4388(93)90169-y)

834 Sparks DL, Barton EJ, Gandhi NJ, Nelson J. Studies of the role of the paramedian pontine  
835 reticular formation in the control of head-restrained and head-unrestrained gaze shifts. *Annals*  
836 *NY Acad Sciences* 956: 85-98, 2002. doi: [10.1111/j.1749-6632.2002.tb02811.x](https://doi.org/10.1111/j.1749-6632.2002.tb02811.x)

837 Sparks DL, Hu X. Saccade initiation and the reliability of motor signals involved in the  
838 generation of saccadic eye movements. In *Novartis Foundation Symposium* (Vol. 270, p. 75).  
839 Chichester; New York; John Wiley 1999, 2006.

840 Sparks DL, Lee C, Rohrer WH. Population coding of the direction, amplitude, and velocity of  
841 saccadic eye movements by neurons in the superior colliculus. *Cold Spring Harb Symp Quant*  
842 *Biol* 55: 805–811, 1990. doi: [10.1101/sqb.1990.055.01.075](https://doi.org/10.1101/sqb.1990.055.01.075)

843 Strassman A, Highstein SM, McGrea RA. Anatomy and physiology of saccadic burst neurons  
844 in the alert squirrel monkey. I. Excitatory burst neurons. *J Comp Neurol* 249: 337–357, 1986a.  
845 doi: [10.1002/cne.902490303](https://doi.org/10.1002/cne.902490303)

846 Strassman A, Highstein SM, McCrea RA. Anatomy and physiology of saccadic burst neurons  
847 in the alert squirrel monkey. II. Inhibitory burst neurons. *J Comp Neurol* 249: 358–380,  
848 1986b. doi: [10.1002/cne.902490304](https://doi.org/10.1002/cne.902490304)

849 Sylvestre PA and Cullen KE. Quantitative analysis of abducens neuron discharge dynamics  
850 during saccadic and slow eye movements. *J Neurophysiol* 82: 2612-2632, 1999. doi:  
851 [10.1152/jn.1999.82.5.2612](https://doi.org/10.1152/jn.1999.82.5.2612)

852 Takagi M, Zee DS, Tamargo RJ. Effects of lesions of the oculomotor vermis on eye  
853 movements in primate: saccades. *J Neurophysiol* 80: 1911-1931, 1998. doi:  
854 [10.1152/jn.1998.80.4.1911](https://doi.org/10.1152/jn.1998.80.4.1911)

855 Takahashi M, Sugiuchi Y, Shinoda Y. Convergent synaptic inputs from the caudal fastigial  
856 nucleus and the superior colliculus onto pontine and pontomedullary reticulospinal neurons. *J*  
857 *Neurophysiol* 111: 849–967, 2014. doi: [10.1152/jn.00634.2013](https://doi.org/10.1152/jn.00634.2013)

858 Ugolini G, Klam F, Doldan Dans M, Dubayle D, Brandi A-M, Büttner-Ennever J, Graf W.  
859 Horizontal eye movement networks in primates as revealed by retrograde transneuronal

860 transfer of rabies virus: differences in monosynaptic input to "slow" and "fast" abducens  
861 motoneurons. J Comp Neurol 20: 498: 762-785, 2006. [10.1002/cne.21092](https://doi.org/10.1002/cne.21092)

862 van Gisbergen JAM, Robinson DA, Gielen S. A quantitative analysis of generation of  
863 saccadic eye movements by burst neurons. J Neurophysiol 45: 417-442, 1981. doi:  
864 [10.1152/jn.1981.45.3.417](https://doi.org/10.1152/jn.1981.45.3.417)

865

866 **Legends of figures**

867 Fig. 1. Effect of unilateral muscimol injection in the caudal fastigial nucleus on tracking a visual  
868 target moving along the vertical meridian. The time course of eye movements produced before  
869 (gray) and after (black) unilateral muscimol injection in the cFN is shown for six different trials.  
870 The eye position (horizontal: upper row; vertical: bottom row) is plotted as a function of time  
871 after target motion onset. The target moved at the constant speed of 20°/s. The selected trials  
872 were recorded during the experiments A2 (A, injection in left cFN) and A3 (B, left cFN) in  
873 monkey A and the experiment Bi9 (C, injection in the right cFN) in monkey Bi.

874

875 Fig. 2. Amplitude-peak velocity relationship of the vertical component of interceptive saccades  
876 toward a target moving along the vertical meridian. This relationship is shown for two  
877 experiments made in each monkey (upper row: A2 and A3 in monkey A; lower row: Bi7 and  
878 Bi8 in monkey Bi), before (gray symbols) and after muscimol injection in the left cFN (black  
879 symbols). The different symbols indicate the different target speeds (●: 10°/s, ■: 20°/s, \*: 40°/s,  
880 ▲: accelerating target, ◆: decelerating target). The number of observations are reported in the  
881 tables 1 and 2.

882

883 Fig. 3. Landing position and time of saccades toward a target moving at constant speed along  
884 the vertical meridian. The vertical (top row) and horizontal (bottom row) landing positions are  
885 plotted as a function of the time after target motion onset when the target moved vertically at  
886 20°/s. Data from before (open symbols) and after (solid symbols) muscimol injection is plotted.  
887 Black and gray symbols correspond to the upward and downward moving target, respectively.  
888 For each monkey, the effects of muscimol injection in the left or right cFN are documented (left  
889 cFN: experiments A3 and Bi7: A-D, right cFN: experiment Bi9: E-F). The dashed line  
890 corresponds to the target position.

891

892 Fig. 4. Position/time landing of saccades toward a target moving at constant speed along the  
893 vertical meridian. The average values of the vertical (panel A) and horizontal (panel B)  
894 components are plotted for the pre- and post-injection sessions of each experiment (square  
895 symbols: monkey A; circle symbols: monkey Bi). The light gray, dark gray and black symbols

896 correspond to the 10, 20 and 40°/s target speeds, respectively. Open and filled symbols  
897 correspond to the upward and downward moving target, respectively. To illustrate the influence  
898 of target speed, the post-injection horizontal average position/time landing of saccades to the  
899 10°/s and 40°/s targets is plotted as a function of the average values obtained with the 20°/s  
900 target (panel C). Diagonal gray lines correspond to equality between abscissae and ordinate  
901 values.

902

903 Fig. 5. Comparing the effects on horizontal and vertical saccades. The post-injection average  
904 values of horizontal position/time landing of vertical saccades are plotted as a function of the  
905 ipsilesional (panel A) and contralesional (panel B) position/time landing of horizontal saccades  
906 (previously described in Bourelly et al. 2018a) for each experiment and each monkey (square  
907 symbols: monkey A; circle symbols: monkey Bi). The panel C shows the horizontal  
908 position/time landing of vertical saccades after muscimol injection as a function of the net  
909 bilateral effect on horizontal saccades (difference of ipsilesional and contralesional horizontal  
910 position/ time landing ratios). The light gray, dark gray and black symbols correspond to the  
911 10, 20 and 40°/s target speeds, respectively. Open and filled symbols correspond to the upward  
912 and downward moving target, respectively.

913

914 Fig. 6. Landing position and time of saccades toward a target moving with a non-constant speed  
915 along the vertical meridian. The horizontal landing positions are plotted as a function of the  
916 landing times for saccades made toward an accelerating (A, B and C) or decelerating (D, E and  
917 F) target, before (open symbols) and after (filled symbols) muscimol injection. Black and gray  
918 symbols correspond to the upward and downward moving target, respectively. The dashed lines  
919 show the horizontal target position.

920

921 Fig. 7. Position/time landing of saccades toward a target moving along the vertical meridian  
922 with a non-constant speed. The average values of the vertical (panel A) and horizontal (panel  
923 B) component were calculated for the pre- and post-injection sessions of each experiment and  
924 plotted for each monkey (square symbols: monkey A; circle symbols: monkey Bi). The gray  
925 and black symbols correspond to the accelerating and decelerating target, respectively. Open  
926 and filled symbols correspond to the upward and downward moving target, respectively. To

927 illustrate the effect of target speed, the post-injection horizontal average position/time landing  
928 of saccades to the accelerating and decelerating targets is plotted as a function of the values  
929 obtained with the 20°/s target (constant speed) (panel C). Diagonal gray lines correspond to  
930 unity lines.

931

932 Fig. 8. Horizontal landing position of saccades toward a target moving along the vertical  
933 meridian. The horizontal landing positions are plotted as a function of the vertical amplitude  
934 after muscimol injection in the left cFN in monkey A (A and B: experiments A2 and A3) and  
935 monkey Bi (C and D: experiments Bi7 and Bi8). The light gray, dark gray and black symbols  
936 correspond to the 10, 20 and 40°/s target speed, respectively. Open and filled symbols  
937 correspond to the upward and downward moving target, respectively. The relation obtained  
938 with saccades toward a target moving with changing speeds are shown in the insets (gray  
939 symbols: constant speeds, black symbols: changing speeds).

940 Fig. 9. Pathophysiology of the ipsipulsion of vertical saccades after muscimol injection in the  
941 right caudal fastigial nucleus. The arrows correspond to excitatory connections whereas the  
942 connecting lines ended by a circle depict inhibitory connections. The gray stain illustrates the  
943 muscimol spread. MR: medial rectus; LR: lateral rectus; MNs: motoneurons; INs: internuclear  
944 neurons; EBns and IBns: excitatory and inhibitory burst neurons; SFNs: saccade-related  
945 fastigial neurons. See text for the detailed explanation of the small letters.

946

947 **Legends of tables**

948 Table 1. Relation between horizontal landing position and both vertical saccade duration and  
949 amplitude after cFN inactivation (target moving at constant speed). Values are the slope, y  
950 intercepts and coefficient of determination of the regression lines that fit the relationship  
951 between the horizontal landing position and the vertical amplitude or duration of saccades  
952 toward a target moving at constant speed (upward and downward movement pooled together).  
953 Injections are labeled as defined in the text. The side and volume of injection are also indicated.  
954 Bold numerical values correspond to statistically significant correlations ( $P < 0.05$ ).

955

956 Table 2. Relation between horizontal landing position and both vertical saccade duration and  
957 amplitude after cFN inactivation (accelerating and decelerating target). Values are the slope, y  
958 intercepts, and coefficient of determination of the regression lines that fit the relationships  
959 between horizontal landing position and the vertical amplitude and duration of saccades toward  
960 a target moving with an increasing speed (from 0 to 40°/s, accelerating target) or decreasing  
961 speed (from 40 to 0°/s, decelerating target). Upward and downward movement are pooled  
962 together. Injections are labeled as defined in the text. The side and volume of injection are also  
963 indicated. Bold numerical values correspond to statistically significant correlations ( $P < 0.05$ ).

964

965

966 **Acknowledgements:**

967 Supported by the Centre National de la Recherche Scientifique, this work received funding  
968 from the European Research Council under the European Union's Seventh Framework  
969 Programme (FP7/2007-2013/ERC grant agreement no. AG324070 with Patrick Cavanagh) and  
970 from the Agence Nationale de la Recherche (Grant VISAFIX). This work was also made  
971 possible thanks to a support from the Fondation pour la Recherche Médicale  
972 (FDT20160435585) to CB, and from the Fondation de France (Berthe Fouassier 0039352) to  
973 JQ. The authors thank Dr Paul May for his corrections and suggestions for clarification, Marc  
974 Martin, Luc Renaud for outstanding zootechnical and surgical assistance, Xavier Degiovanni  
975 and Joël Baurberg for technical assistance, Ivan Balansard for veterinarian surveillance, and Dr  
976 Ivo Vanzetta for kindly lending us one monkey (Bi).

Fig. 1

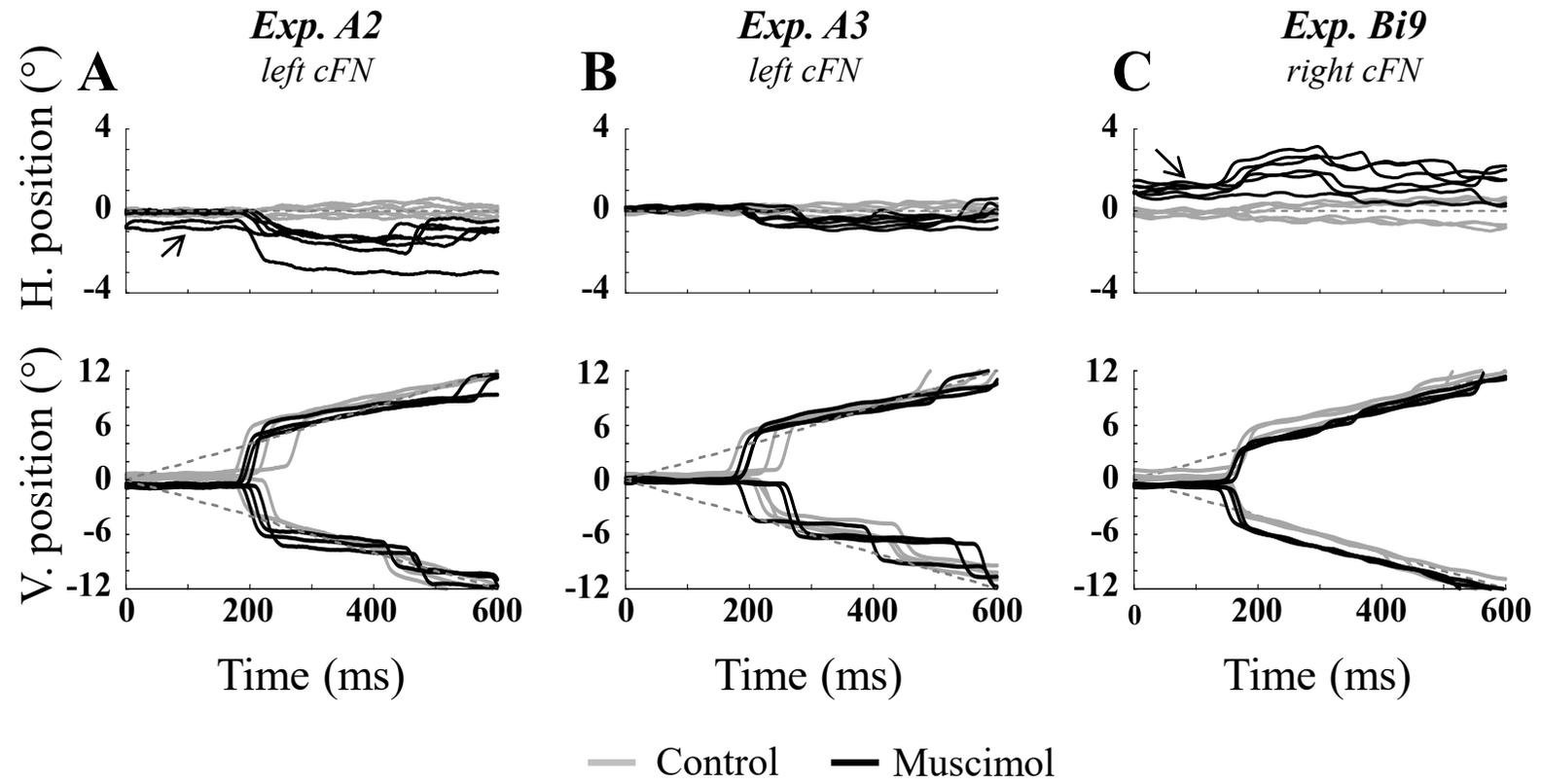


Fig. 2

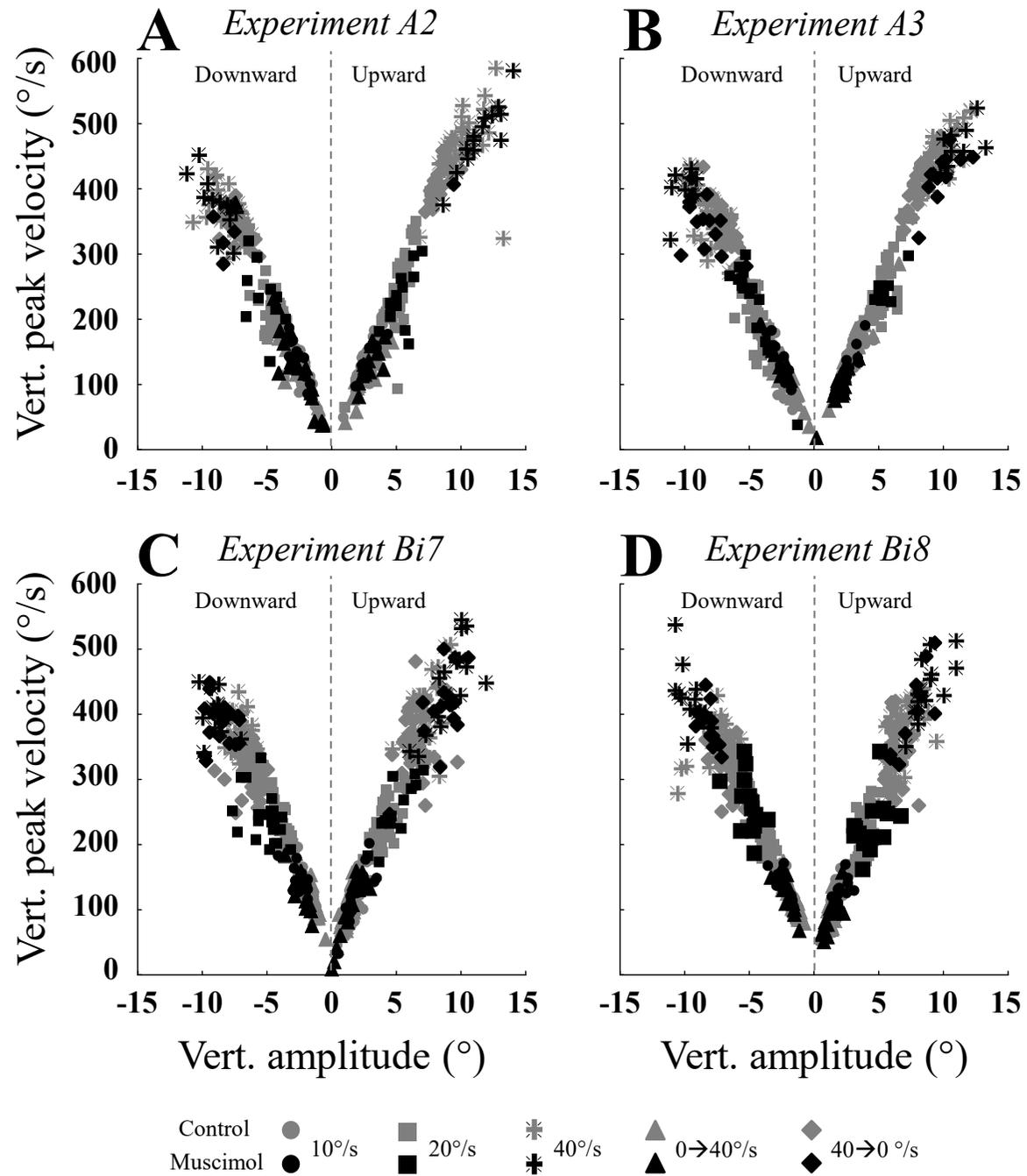


Fig. 3

# Constant target speed

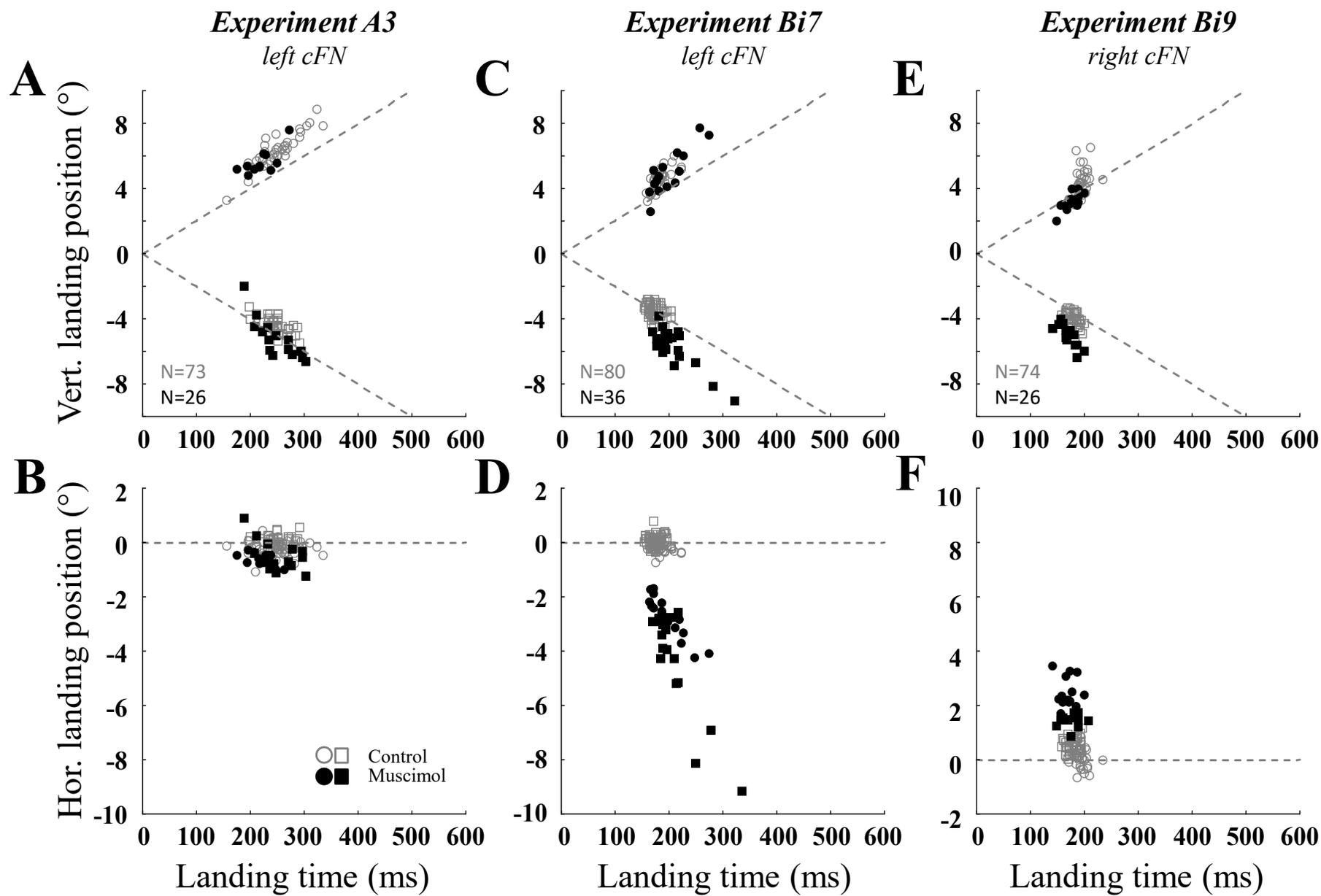




Fig. 5

## Constant target speed

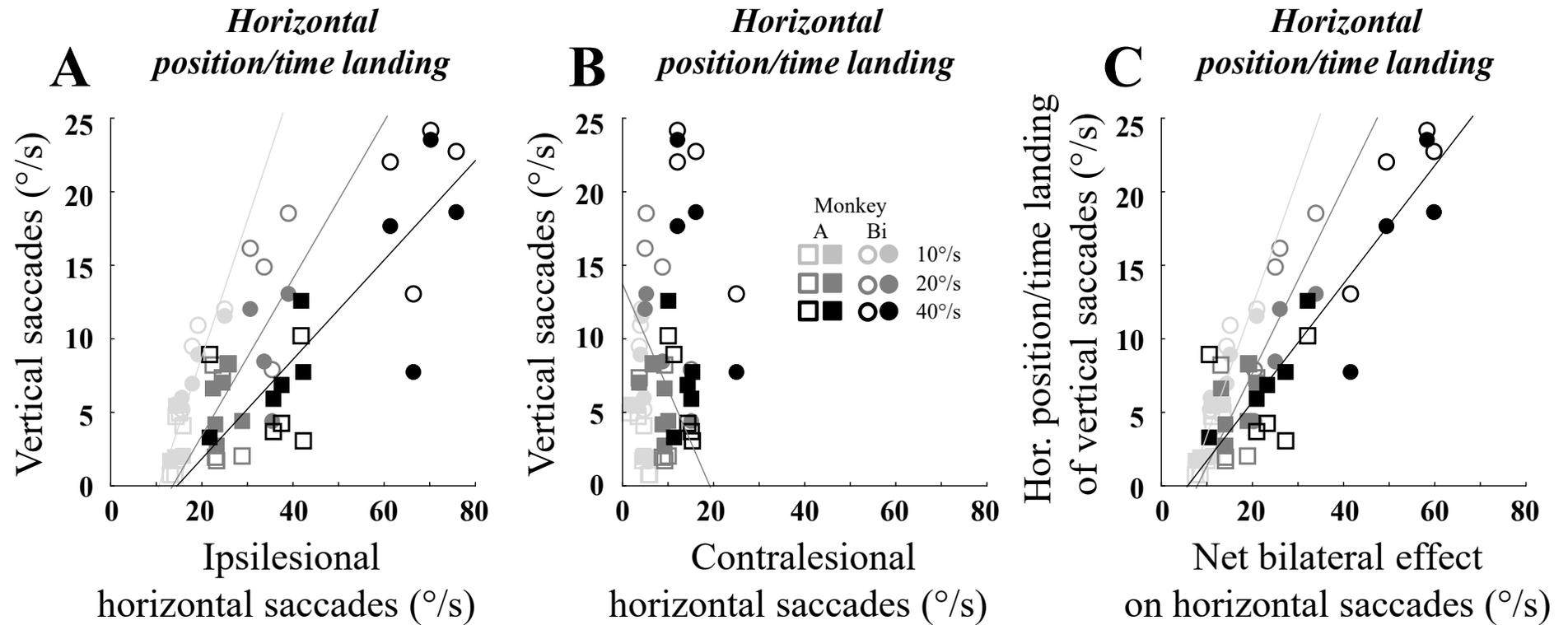


Fig. 6

## Changing target speed

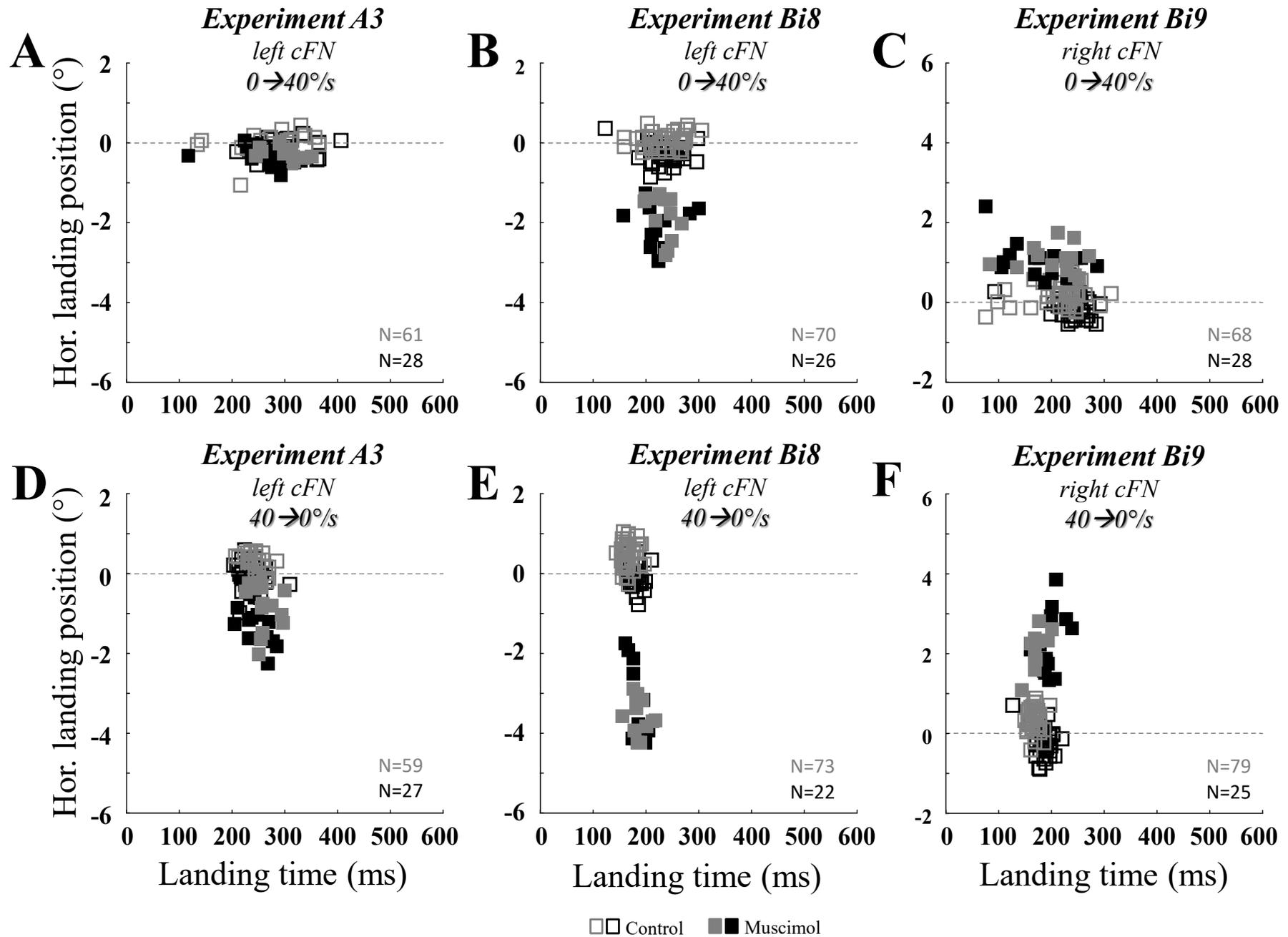


Fig. 7

## Changing target speed

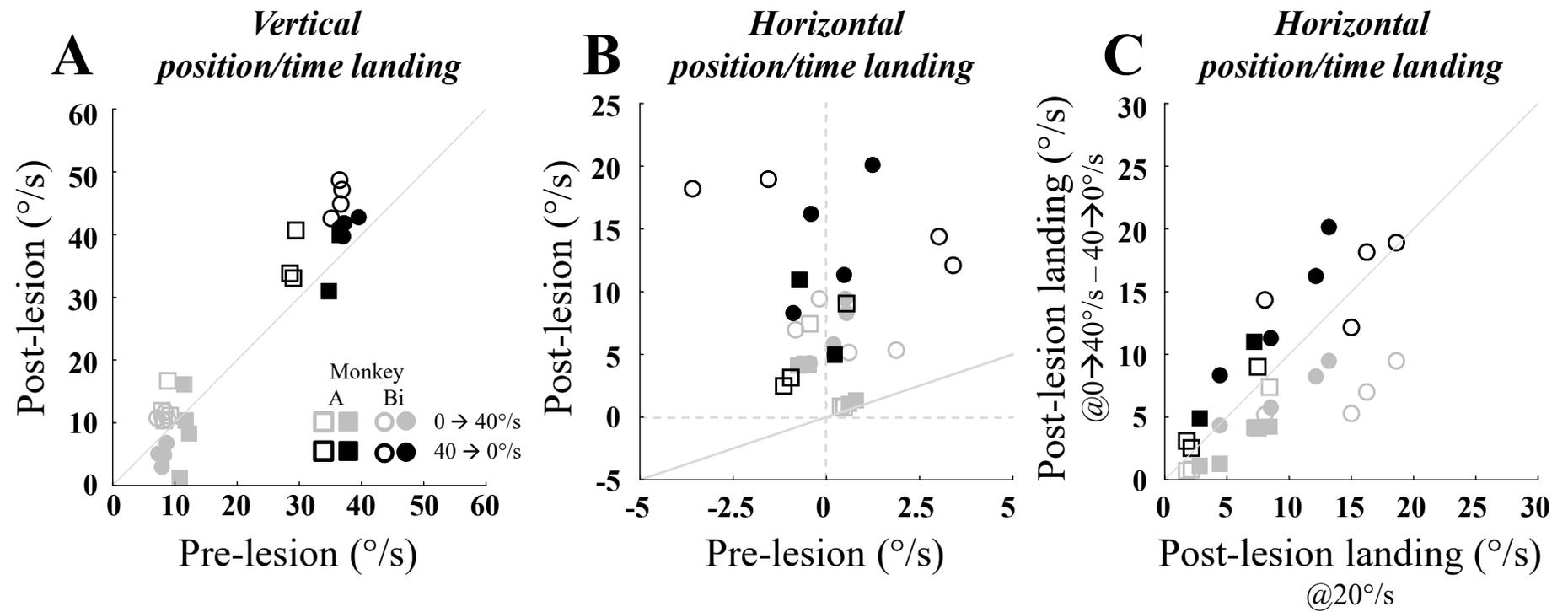


Fig. 8

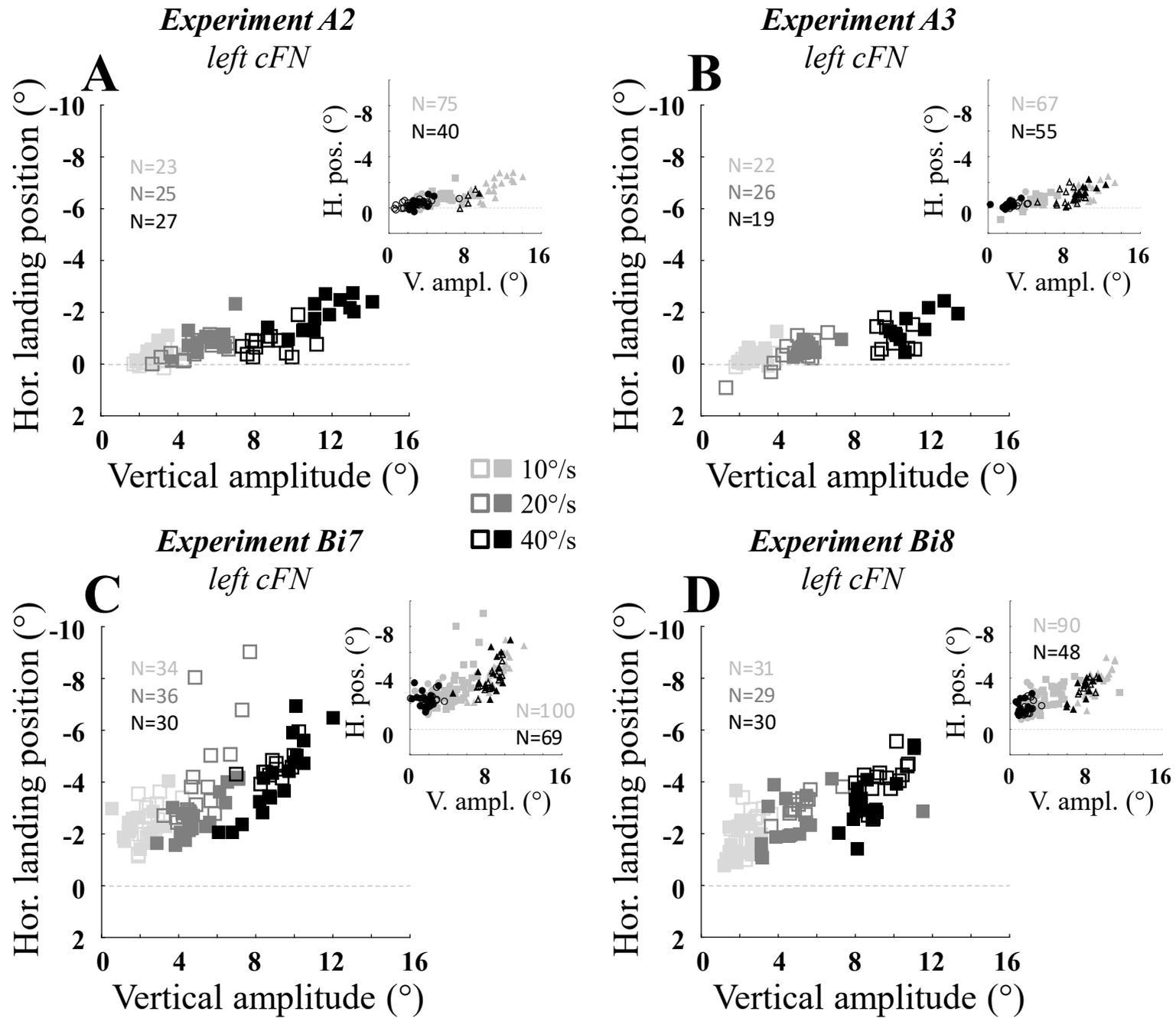
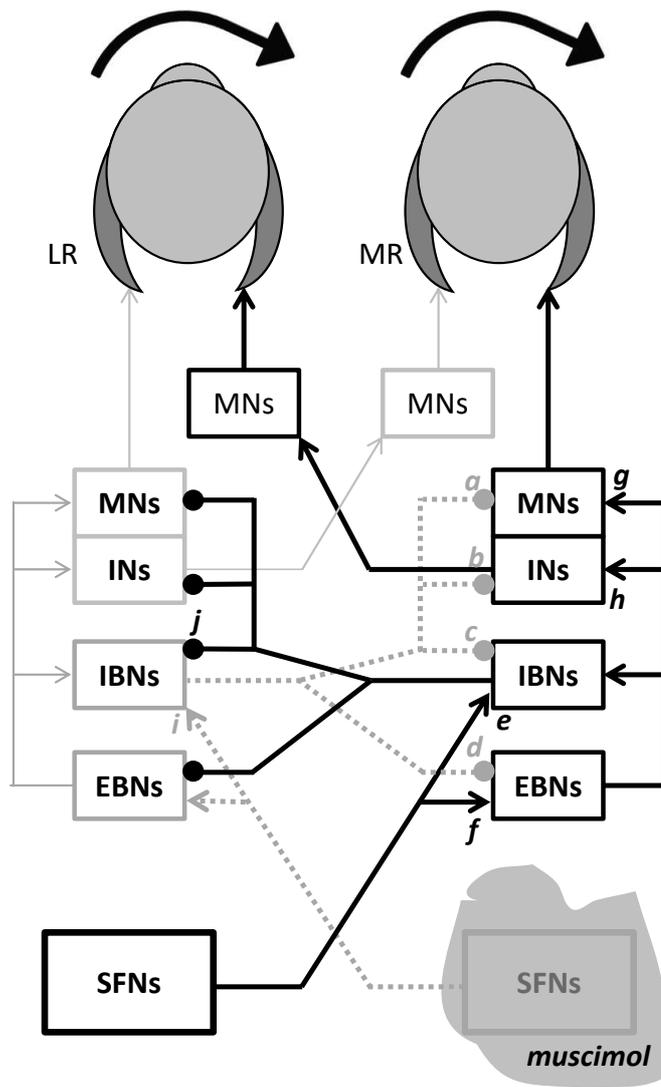


Figure 9



# Table 1

Exp	injection		10°/s				20°/s				40°/s			
			N	Y-int	slope	R <sup>2</sup>	N	Y-int	slope	R <sup>2</sup>	N	Y-int	slope	R <sup>2</sup>
A1	Left cFN 1.0 µl	Amplitude	18	-0.2	-0.108	0.09 NS	<b>38</b>	<b>-0.0</b>	<b>-0.132</b>	<b>0.26*</b>	<b>20</b>	<b>1.1</b>	<b>-0.239</b>	<b>0.48*</b>
		Duration	18	-0.5	-0.001	0.001 NS	<b>38</b>	<b>0.3</b>	<b>-0.028</b>	<b>0.14*</b>	<b>20</b>	<b>1.6</b>	<b>-0.067</b>	<b>0.52*</b>
A2	Left cFN 0.5 µl	Amplitude	23	0.2	-0.185	0.15 NS	<b>25</b>	<b>0.7</b>	<b>-0.281</b>	<b>0.42*</b>	<b>27</b>	<b>1.9</b>	<b>-0.327</b>	<b>0.65*</b>
		Duration	23	-0.1	-0.009	0.01 NS	25	-0.2	-0.014	0.07 NS	<b>27</b>	<b>1.5</b>	<b>-0.065</b>	<b>0.17*</b>
A3	Left cFN 0.3 µl	Amplitude	<b>22</b>	<b>0.4</b>	<b>-0.278</b>	<b>0.33*</b>	<b>26</b>	<b>1.1</b>	<b>-0.328</b>	<b>0.66*</b>	<b>19</b>	<b>1.7</b>	<b>-0.284</b>	<b>0.29*</b>
		Duration	22	0.4	-0.024	0.10 NS	26	0.6	-0.031	0.06 NS	19	-1.0	-0.005	0.003 NS
A4	Right cFN 1.1 µl	Amplitude	30	1.3	0.055	0.001 NS	26	2.4	-0.062	0.003 NS	-	-	-	-
		Duration	30	-0.9	0.070	0.08 NS	26	0.7	0.034	0.03 NS	-	-	-	-
A5	Right cFN 1.0 µl	Amplitude	<b>15</b>	<b>2.5</b>	<b>-0.411</b>	<b>0.29*</b>	28	1.5	0.044	0.00 NS	<b>18</b>	<b>5.7</b>	<b>-0.413</b>	<b>0.31*</b>
		Duration	15	3.1	-0.069	0.10 NS	28	1.5	0.005	0.00 NS	18	1.9	-0.007	0.002 NS
A6	Right cFN 0.5 µl	Amplitude	<b>26</b>	<b>0.6</b>	<b>0.252</b>	<b>0.18*</b>	<b>24</b>	<b>0.5</b>	<b>0.207</b>	<b>0.26*</b>	<b>26</b>	<b>-0.1</b>	<b>0.312</b>	<b>0.53*</b>
		Duration	26	0.5	0.026	0.13 NS	24	0.8	0.019	0.11 NS	<b>26</b>	<b>-0.1</b>	<b>0.066</b>	<b>0.36*</b>
Bi7	Left cFN 0.2 µl	Amplitude	<b>34</b>	<b>-1.6</b>	<b>-0.355</b>	<b>0.15*</b>	<b>36</b>	<b>1.0</b>	<b>-0.889</b>	<b>0.41*</b>	<b>30</b>	<b>2.6</b>	<b>-0.772</b>	<b>0.67*</b>
		Duration	<b>34</b>	<b>-0.5</b>	<b>-0.078</b>	<b>0.28*</b>	<b>36</b>	<b>3.2</b>	<b>-0.198</b>	<b>0.37*</b>	30	-1.8	-0.066	0.09 NS
Bi8	Left cFN 0.2 µl	Amplitude	<b>31</b>	<b>-0.9</b>	<b>-0.522</b>	<b>0.18*</b>	<b>29</b>	<b>-1.7</b>	<b>-0.209</b>	<b>0.18*</b>	<b>30</b>	<b>2.7</b>	<b>-0.701</b>	<b>0.56*</b>
		Duration	<b>31</b>	<b>0.1</b>	<b>-0.088</b>	<b>0.30*</b>	<b>29</b>	<b>-0.5</b>	<b>-0.073</b>	<b>0.28*</b>	<b>30</b>	<b>-0.6</b>	<b>-0.078</b>	<b>0.14*</b>
Bi9	Right cFN 0.5 µl	Amplitude	<b>24</b>	<b>0.8</b>	<b>0.338</b>	<b>0.22*</b>	<b>26</b>	<b>-0.2</b>	<b>0.576</b>	<b>0.34*</b>	24	3.1	0.061	0.00 NS
		Duration	24	1.0	0.021	0.07 NS	26	-0.3	0.081	0.11 NS	24	3.4	0.006	0.00 NS
Bi10	Right cFN 0.2 µl	Amplitude	28	1.3	-0.130	0.02 NS	<b>28</b>	<b>-0.3</b>	<b>0.351</b>	<b>0.23*</b>	26	0.8	0.120	0.02 NS
		Duration	28	0.5	0.023	0.06 NS	28	0.7	0.013	0.01 NS	26	2.0	-0.005	0.00 NS

## Table 2

Exp	injection		Accelerating target				Decelerating target			
			N	Y-int	slope	R <sup>2</sup>	N	Y-int	slope	R <sup>2</sup>
A2	Left cFN 0.5 µl	Amplitude	<b>35</b>	<b>0.0</b>	<b>-0.131</b>	<b>0.34*</b>	5	4.9	-0.663	0.74 NS
		Duration	35	0.0	-0.012	0.06 NS	5	-0.8	0.001	0.00 NS
A3	Left cFN 0.3 µl	Amplitude	<b>28</b>	<b>-0.0</b>	<b>-0.104</b>	<b>0.18*</b>	<b>27</b>	<b>1.1</b>	<b>-0.233</b>	<b>0.31*</b>
		Duration	<b>28</b>	<b>0.2</b>	<b>-0.016</b>	<b>0.15*</b>	27	-0.5	-0.012	0.04 NS
A4	Right cFN 1.1 µl	Amplitude	15	2.7	-0.196	0.10 NS	-	-	-	-
		Duration	15	3.1	-0.034	0.06 NS	-	-	-	-
A6	Right cFN 0.5 µl	Amplitude	<b>24</b>	<b>0.7</b>	<b>0.215</b>	<b>0.29*</b>	<b>27</b>	<b>0.4</b>	<b>0.231</b>	<b>0.39*</b>
		Duration	24	0.4	0.026	0.14 NS	27	1.1	0.027	0.14 NS
Bi7	Left cFN 0.2 µl	Amplitude	35	-2.3	0.016	0.00 NS	<b>34</b>	<b>0.9</b>	<b>-0.581</b>	<b>0.34*</b>
		Duration	35	-1.8	-0.019	0.04 NS	<b>34</b>	<b>-0.7</b>	<b>-0.088</b>	<b>0.25*</b>
Bi8	Left cFN 0.2 µl	Amplitude	26	-1.4	-0.205	0.06 NS	<b>22</b>	<b>1.5</b>	<b>-0.594</b>	<b>0.55*</b>
		Duration	<b>26</b>	<b>-0.4</b>	<b>-0.063</b>	<b>0.32*</b>	22	-1.3	-0.052	0.10 NS
Bi9	Right cFN 0.5 µl	Amplitude	28	1.0	0.013	0.00 NS	<b>25</b>	<b>-0.3</b>	<b>0.310</b>	<b>0.33*</b>
		Duration	28	1.0	0.002	0.00 NS	<b>25</b>	<b>0.7</b>	<b>0.039</b>	<b>0.17*</b>
Bi10	Right cFN 0.2 µl	Amplitude	29	0.9	0.115	0.04 NS	<b>22</b>	<b>-2.2</b>	<b>0.537</b>	<b>0.12*</b>
		Duration	29	0.7	0.016	0.04 NS	22	3.7	-0.04	0.05 NS